inter.noise
HAMBURG 2016

Toward Reduced Aircraft Community Noise Impact via a Perception-Influenced Design Approach

Stephen A. RIZZI[1]

[1] NASA Langley Research Center, Hampton, Virginia, USA

ABSTRACT

This is an exciting time for aircraft design. New configurations, including small multi-rotor uncrewed aerial systems, fixed- and tilt-wing distributed electric propulsion aircraft, high-speed rotorcraft, hybrid-electric commercial transports, and low-boom supersonic transports, are being made possible through a host of propulsion and airframe technology developments. The resulting noise signatures may be radically different, both spectrally and temporally, than those of the current fleet. Noise certification metrics currently used in aircraft design do not necessarily reflect these characteristics and therefore may not correlate well with human response. Further, as operations and missions become less airport-centric, e.g., those associated with on-demand mobility or package delivery, vehicles may operate in closer proximity to the population than ever before. Fortunately, a new set of tools are available for assessing human perception during the design process in order to affect the final design in a positive manner. The tool chain utilizes system noise prediction methods coupled with auralization and psychoacoustic testing, making possible the inclusion of human response to noise, along with performance criteria and certification requirements, into the aircraft design process. Several case studies are considered to illustrate how this approach could be used to influence the design of future aircraft.

Keywords: Aircraft Community Noise, Human Perception, Design
I-INCE Classification of Subjects Numbers: 13.1, 66.2

1. INTRODUCTION

Human response to aircraft community noise is a complex perception phenomenon that is a function of both transportation-mode-specific acoustic (1) and non-acoustic factors (2). The aircraft vehicle design process requires a multidisciplinary approach to achieve a set of design goals that typically includes performance, emissions, fuel/energy consumption, and noise. Noise goals used in aircraft design are usually specified in terms of certification metrics, which may not fully reflect acoustic factors related to human response, nor are intended to reflect non-acoustic factors. The International Civil Aviation Organization (ICAO) has adopted a set of noise certification requirements, specified in Annex 16, Volume I (3), as part of a balanced approach to aircraft noise management (4), with a focus on airport environments. In addition to noise certification requirements, other facets of the balanced approach include land-use planning and management, noise abatement operational procedures, and operating restrictions. The fourteen chapters in part II of ref. (3) deal with certification of prior, current and future aircraft. Regulatory authorities in the member states implement these requirements, e.g., the Federal Aviation Administration (FAA) in the U.S. has implemented compatible noise certification requirements in Federal Aviation Regulation (FAR) Part 36 (5) and the European Aviation Safety Agency (EASA) through Regulation (EC) No. 216/2008 Article 6 (6), as amended by Commission Regulation (EU) 2016/4.

A common misconception is that the ICAO attempts to promote aircraft noise reduction through increasingly stringent noise requirements. Noise requirements have never forced the development of new technology, nor has a rule been put in place that required the use of unproven technology. This philosophy is embodied in the ICAO balanced approach which strives to manage aircraft noise "in the most cost-effective manner," as well as by the FAA which stipulates in FAR 36 that "the noise levels in this part have been determined to be as low as is economically reasonable, technologically practicable, and appropriate to the type of aircraft to which they apply." FAR 36 further states that

[1] stephen.a.rizzi@nasa.gov

"No determination is made, under this part, that these noise levels are or should be acceptable or unacceptable for operation at, into, or out of, any airport." In other words, current noise certification regulations do not ensure that the noise exposure is, by any definition, acceptable. On the contrary, it is the action of selected airport authorities, e.g., London Heathrow Airport (7), which have put in place restrictions and tariffs to promote the use of the best equipment in response to community opposition to noise. It is because of such economic pressure that operators insist on improved technology from the aircraft manufacturers so that they may be allowed to profitably operate in these critical localities. Over time, this changes what is considered to be economically reasonable and technologically practicable. The fact that noise certification requirements have become more stringent over time, e.g., for subsonic jet aircraft from chapter 2 to 3 to 4, and by 2017 and 2020, to chapter 14, is therefore a reaction to the current technology, and the notion of preventing backsliding. In this respect, vehicle noise design is mainly driven by stringent local noise requirements, to a lesser extent by regulatory agencies, and even less so by averaged metrics used in land-use planning.

It is quite likely that aircraft noise design will continue to be based solely on acoustical factors for the foreseeable future. However, given that the current certification requirements are not focused on achieving low annoyance designs, it is worth considering how other acoustical factors contributing to annoyance might be incorporated in the design process. In other words, is it possible to achieve reduced community noise impact by simultaneously meeting noise certification and other design requirements (e.g., fuel burn and emissions), along with other requirement(s), which directly address human response, whether they be related to annoyance, sleep disturbance, speech interference, audibility, etc., or some combination thereof? This paper puts forth the proposition that it is possible to do so through a perception-influenced design approach.

Perception-influenced design (PID) for noise is the process by which the engineering design is affected, in a positive manner, by human perception. In aircraft noise design, PID is made possible through a new set of tools for system noise prediction, coupled with auralization and psychoacoustic testing. In some cases, it may be that suitable noise metrics exist, in which case the design process can be performed using that metric as a cost functional without the necessity for separate human response testing. For example, it is not unreasonable to assume that low annoyance designs of conventional turbofan-driven tube-and-wing commercial transports could be achieved, to a degree, using the effective perceived noise level certification metric as a surrogate for a more direct annoyance metric cost functional, since annoyance to such sounds are supposed to be reflected in the underlying perceived noise level (8). However, new aircraft configurations, including small multi-rotor uncrewed aerial systems (UAS), fixed- and tilt-wing distributed electric propulsion aircraft, high-speed rotorcraft, hybrid-electric commercial transports, and low-boom supersonic transports, are now on the drawing boards. These designs are being made possible through a host of propulsion and airframe technology developments, and the resulting noise signatures may be radically different, both spectrally and temporally, than aircraft comprising the current fleet. In these cases, current certification metrics, which do not generally reflect these characteristics, may not correlate well with human response. Further, as operations and missions become less airport-centric, e.g., those associated with on-demand mobility or package delivery, vehicles may operate in closer proximity to the population and for longer durations than ever before. Therefore, other psychoacoustic metrics, which are known to correlate with the desired human response, may serve as the cost functional. When such metrics do not exist, or when their correlation with the offending noise source is not known, laboratory studies, based on auralization of system noise predictions, may be used to identify or develop an appropriate metric or even use the response data directly in the absence of a metric. It is in these ways that PID can move toward reduced aircraft community noise impact by affecting the vehicle design.

In the remainder of this paper, the aircraft noise certification metrics currently employed for the majority of flight vehicles are first reviewed. Next, the elements of PID are discussed in a general sense, and its application is explored in case studies of four vehicles of interest; a large commercial transport with a desired target sound, a distributed electric propulsion system employing a propeller-driven high-lift system, a hybrid wing body which takes advantage of propulsion airframe aeroacoustics and advanced noise reduction technology to achieve its noise reduction, and a low-boom supersonic aircraft.

2. REVIEW OF AIRCRAFT NOISE CERTIFICATION METRICS

It is helpful to review the single-event aircraft noise certification metrics in use today as these typically serve as the starting point in the design process. A compendium of aircraft noise metrics is provided by Bennett and Pearsons (9).

2.1 Maximum A-Weighted Sound Pressure Level

The noise certification metric used for lightweight propeller-driven aircraft with a certified takeoff mass not exceeding 8618 kg is the maximum A-weighted sound pressure level (SPL), slow response, relative to 20μPa, designated by L_{Amax} (dBA). Takeoff procedures are described in Chapter 10 (3). The maximum allowable levels are a function of the maximum certificated takeoff mass. The Chapter 10 noise requirements affect all propeller-driven aircraft below 8618 kg, irrespective of their size, mass and use. At least two small uncrewed aerial systems have been certified in the United States under FAR 36, Appendix G; the analog to Chapter 10.

The frequency weighting in L_A adjusts the actual decibel level to a scale matching the level perceived by the human ear, according to a single equal loudness contour, using the measurement method prescribed in Appendix 6 (3). The duration of the event does not influence L_{Amax}.

2.2 Sound Exposure Level

Another metric used for aircraft certification is the sound exposure level (SEL), designated by L_{AE} (dBA). This metric applies to lightweight helicopters not exceeding 3175 kg, and is applied to a straight and level flyover flight test procedure at 150 m above ground level, as described in Chapter 11 (3). Maximum allowable levels for light helicopters are also a function of the maximum certificated takeoff mass.

SEL takes into account both level and duration and in discrete form is given by

$$L_{AE} = 10\log_{10}\frac{1}{T_0}\sum_{k_F}^{k_L} 10^{0.1L_A(k)}\Delta t \tag{1}$$

in which T_0 is the reference integration time of 1 s, $L_A(k)$ is the time-varying A-weighted SPL at the k^{th} instant of time, Δt is the time increment between samples. When used for certification, k_F and k_L are the first and last increments of k between the period when $L_A(k)$ first rises to 10 dBA below L_{Amax} and falls below the last value of 10 dBA below L_{Amax}, respectively. All else being equal, a doubling of duration increases SEL by 3 dBA.

2.3 Effective Perceived Noise Level

The effective perceived noise level (EPNL) is used for certification of a host of other aircraft configurations. New aircraft are certified according to:

- Chapter 4 – subsonic jet aircraft over 55000 kg (certification applied between 2006-17), subsonic jet aircraft less than 55000 kg (certification applied between 2006-20), and propeller-driven aircraft between 8618-55000 kg (certification applied between 2006-20),
- Chapter 7 – propeller-driven short takeoff and landing (STOL) aircraft over 5700 kg (guidelines only)
- Chapter 8 – helicopters (lightweight helicopters under 3175 kg may certify under either Chapter 8 or 11),
- Chapter 12 – supersonic aircraft after 1975 (not developed),
- Chapter 13 – tilt-rotors (certification applied after 2018),
- Chapter 14 – subsonic jet and propeller-driven aircraft over 55000 kg (certification applied after 2017), subsonic jet aircraft less than 55000 kg (certification applied after 2020), and propeller-driven aircraft between 8618-55000 kg (certification applied after 2020).

Maximum allowable EPNL levels (EPNdB) are aircraft configuration-, weight-, and number of engine- (Chapters 4 & 14) dependent. The reader is referred to Attachment A of ref. (3) for details. For each of the aircraft configurations indicated above, three certification points are utilized. For Chapter 4 and 14 aircraft, these are the approach, lateral (also called takeoff or sideline), and flyover (also called cutback) conditions, as shown in Figure 1. Helicopters covered under Chapter 8 use approach, takeoff, and overflight certification points (not shown).

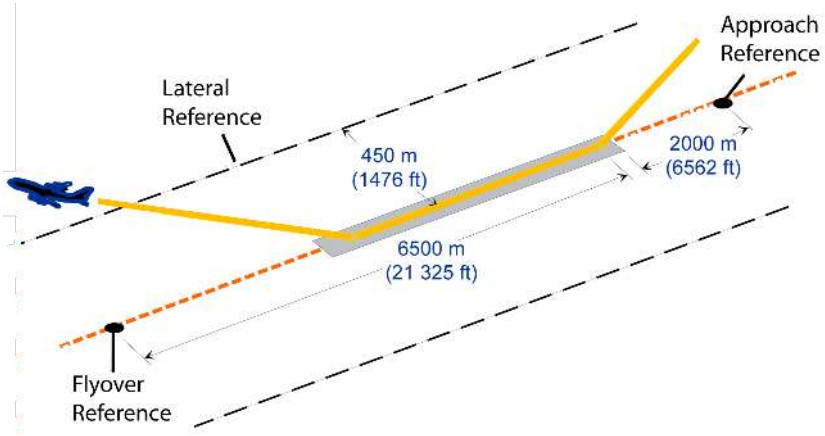

Figure 1 – Certification points for Chapters 4 and 14 aircraft.

The EPNL metric is calculated through a multi-step process summarized below. The reader is referred to Appendix 2 of ref. (3) for details. The process starts with the measurement of one-third octave band SPL spectra, in 24 bands from 50 Hz to 10 kHz, at a time increment Δt of 0.5 s. At each time interval k, the SPL spectrum is first converted to a perceived noisiness spectrum, expressed in noy. A weighted sum is taken to obtain the perceived noise level at the k^{th} time increment, PNL(k), expressed in PNdB. Next, a tone correction, based on the maximum difference between adjacent one-third octave bands of SPL(k), is applied to PNL(k) to obtain the tone-corrected perceived noise level PNLT(k), also expressed in PNdB. The tone-correction increases with level difference, and is higher within the more sensitive human hearing range between 500 Hz and 5 kHz. EPNL is calculated as the logarithmic sum of PNLT values over the event duration, e.g., approach, according to

$$EPNL = 10\log_{10}\left[\left(\frac{1}{T}\right)\sum_{k=0}^{d/\Delta t}\Delta t\, 10^{\left(\frac{PNLT(k)}{10}\right)}\right] \tag{2}$$

in which T is a normalizing time constant of 10s, and d is the time interval to the nearest 0.5 s during which PNLT(k) remains greater or equal to $PNLT_{max}$-10. In this manner, the EPNL metric takes into account amplitude, duration, and spectral content.

2.4 Perceived Level

As indicated above, a certification metric for sonic boom of supersonic aircraft has yet to be adopted. A noise metric which has proven to be useful, however, is the Perceived Level (PL), see Section 4.4. There are no standards for computing PL for sonic booms. However, Shepherd and Sullivan (10) adopted Stevens' Mark VII loudness method (11), which extends equal loudness contours to very low frequency (1 Hz), for the calculation of PL for sonic booms. Specifically, since sonic booms are transient in nature, the authors developed an approach to convert the narrowband energy spectral density of the boom signature to one-third octave band sound pressure levels, required as input to Stevens' method, using a procedure recommended by Johnson and Robinson (12) that accounts for the critical time of the human auditory system. A change in PL of 9 dB represents a halving, or doubling, of loudness.

3. DESIGN FOR NOISE

The notion of affecting aircraft design in a significant way to achieve low noise is not new. The introduction of high bypass ratio turbofans in the 1970s is an example of how noise and fuel burn considerations made a significant impact on aircraft design. The more aggressive the goal, the more significant the design change. For example, the noise reduction goals of the National Aeronautics and Space Administration (NASA) Quiet Aircraft Technology (QAT) project in the early 2000s was to reduce by one half (10 EPNdB) the perceived community noise within ten years, and by three quarters (20 EPNdB) within twenty-five years at each certification point (13). It was recognized at that time that significant changes in the aircraft configuration, like the Hybrid Wing Body (HWB), would be required to make this step change in aircraft noise. The ability to simultaneously design for aggressive low noise, emissions, and fuel burn (14, 15), or introduce new vehicle classes and/or

operations, e.g., on-demand aviation (16), is even more challenging. It is one that not only requires multidisciplinary design and optimization, but often necessitates methods development and experimental databases when solutions extend beyond the knowledgebase. Two approaches to design for noise are next discussed. The first describes a multidisciplinary process with noise reduction goals expressed in terms of noise certification levels. The second complements the first and allows the design to also be influenced by human perception beyond certification metrics.

3.1 Metrics-Driven Design Process

Low-noise aircraft design can be implemented at the subcomponent (e.g., low-noise rotor), the component (e.g., propulsor architecture), and at the integrated system (e.g., aircraft configuration) levels. Just as with any other product design, the required engineering toolset and level of fidelity associated with tools in that toolset is dependent on the particular task at hand. Common elements are depicted in Figure 2. In most cases, the starting point for the noise analysis is a description of the isolated source noise at the component level, as shown in the leftmost block. For example, in the design of a large commercial transport, these would include isolated engine (e.g., jet, fan tonal and broadband, and core), and airframe (e.g., landing gear, flaps, and slats) subcomponent source noise prediction models and/or data. Other aircraft types would use source noise component models/data particular to their applications, e.g., main and tail rotor thickness and loading noise for helicopters, tonal and broadband noise for propeller-driven aircraft, etc. Source noise reduction methods might also be applied here, e.g., nacelle liners for fan inlet noise or chevrons for jet noise.

The effects of installation of the sources on the airframe are extremely important when considering the noise of the aircraft system. These are represented by the second block and are referred to as propulsion airframe aeroacoustics (PAA). PAA includes both aerodynamic effects, which modify the source noise generation, e.g., the effect of a pylon on a pusher propeller design, and acoustic effects, which modify the noise propagation, e.g., acoustic shielding of engine sources on a hybrid wing body configuration. The isolated sources and installation effects are brought together in a system noise prediction tool that, whether in an integrated fashion or not, propagates the noise from the source to a ground receiver. Examples include NASA Aircraft Noise Prediction Program (ANOPP) (17) and ANOPP2 (18), the German Aerospace Center (DLR) Parametric Aircraft Noise Analysis Module (PANAM) (19), and the French Aerospace Agency (ONERA) CARMEN acoustic model (20), to name a few.

Of course, other design factors, such as aerodynamic performance, fuel burn, emissions, safety, etc. must be taken into account. These are represented by the multidisciplinary analysis and optimization (MDAO) block in Figure 2. The MDAO process will optimize the vehicle design to minimize cost functional(s) within the constraints of each of the constituent design elements, e.g., performance, emissions, acoustics, cost, etc. The cost functional for acoustics is typically taken as the noise certification metric, which is computed from the predicted noise at the ground receiver under the certification flight condition. The feedback loops between the system noise prediction to the PAA and source noise models blocks represent iteration(s) required to close the design.

The metrics-driven design process described above works well for ensuring that new aircraft will meet noise certification requirements. However, it sometimes falls short of achieving low community noise impact. This is the case when the certification metrics don't correlate well with human response, or when the aircraft source noise signatures or their operations change in such a way that the metrics were never intended to capture. Finally, there may be cases when there are no noise certification metrics in place, e.g., sonic boom. In these cases, a perception-influenced design approach may be beneficial.

3.2 Perception-Influenced Design

Perception-influenced design, or alternatively perception-based engineering (21), is the incorporation of human perception into engineering design to achieve a more favorable product. In general, human perception may be affected by sensory and non-sensory, e.g., societal, factors. In acoustics, the idea of integrating human perception into product design is not new. Product sound quality has been applied to different consumer products for many years (22), especially in the automotive industry (23), and can also address both acoustic and non-acoustic factors. Application of these ideas to aircraft design, however, is a recent development and is only beginning to be explored. In the present context, perception-influenced design is meant to address only acoustic factors.

Because the focus is design of future aircraft not yet in service, stimuli for human response testing must be, in some fashion, simulated. This could be accomplished through modification of a recording

from a similar aircraft in service, but such a process is made difficult as one is generally unable to separate the sources. More commonly, the received sound at an observer on the ground is generated through auralization of the system noise prediction, as shown in Figure 2. In this paper, auralization refers to the process by which aircraft noise predictions at the source are transformed into pressure time histories, or pseudo-recordings, at the observer. There are at least two approaches for auralization. One approach entails propagating the source in the frequency domain, then synthesizing the pressure time history at the observer. The second entails synthesizing the pressure time history at the source, then propagating that in the time domain to the observer. Aircraft auralization methods have advanced significantly in recent years, with applications including small UAS (24), propeller-driven aircraft (25), rotorcraft (26), and large commercial transports (27-34). Many more examples exist in the literature.

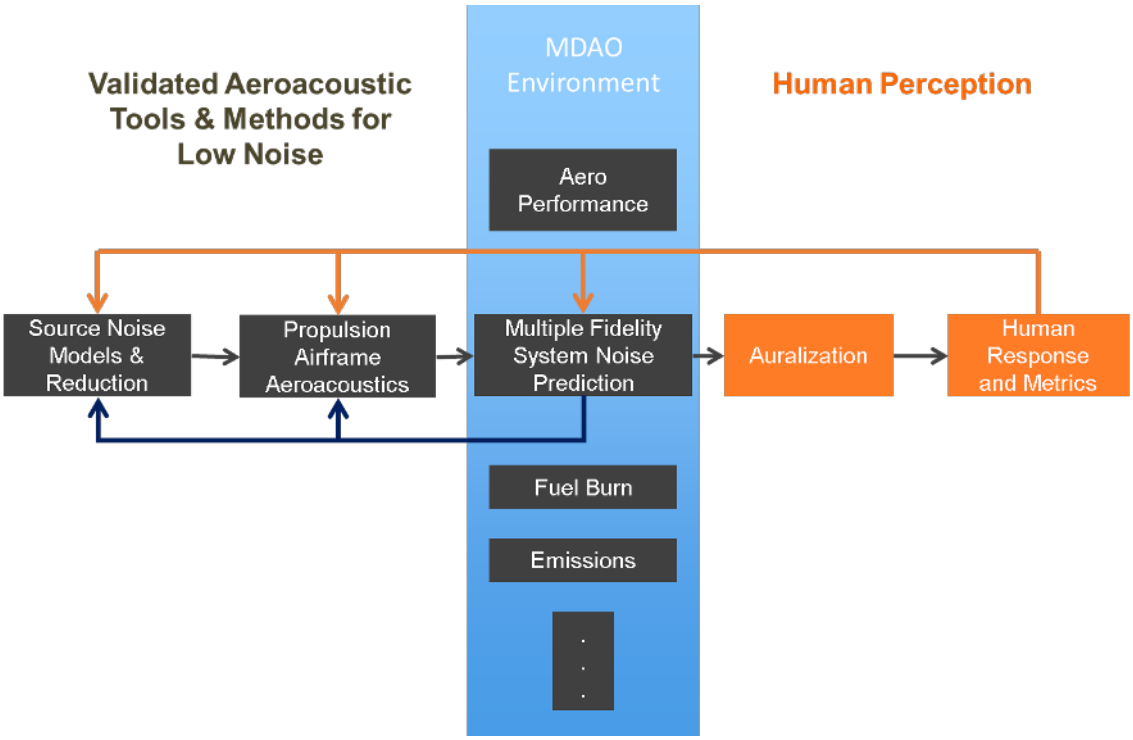

Figure 2 – Components of metrics-driven (black) and perception-influenced (orange) design approaches applied to low-noise aircraft design.

Through the appropriate means of sound reproduction, the auralizations can be used in whole or in part to characterize human response in the form of annoyance, audibility, sleep disturbance, etc. The data acquired from these tests may be used to determine the applicability of existing metrics or develop new metrics, if needed. These metrics can serve as additional cost functionals in the MDAO process, as indicated by the feedback loop from the human response and metrics block to the MDAO block in Figure 2. From there on, the aircraft can be designed for low noise impact according to the metrics-driven design process. In some cases, it may be more expedient to affect the design by providing feedback directly to the source noise modeling and PAA blocks. A seldom mentioned benefit of this tool chain is that it can also be used to identify modeling deficiencies when auralizations of aircraft in the current fleet do not reflect real life experience.

4. CASE STUDIES

Four case studies of PID are next considered. The first case study was one of the first in which researchers attempted to modify the aircraft design to achieve low annoyance. The second is for a propeller-driven aircraft, which has noise signatures that differ substantially from other aircraft in that class. The third is for a turbofan-driven large commercial aircraft, where a multidisciplinary design was developed using its noise certification metric as one of the cost functionals. The last case is for a low-boom supersonic aircraft for which a sonic boom certification metric does not yet exist.

4.1 SEFA/COSMA Projects

In the last twelve years, two European Commission framework projects have essentially been devoted to low annoyance aircraft design. The 2004-07 FP6 project, Sound Engineering For Aircraft (SEFA) (35), had as one of its objectives the identification of desirable sound attributes. Using these as target sounds, a sound-matching-based cost functional was developed for use in a multidisciplinary conceptual design optimization where the difference between a 'weakly annoying' target sound, identified with a sound engineering method (36, 37), and the predicted sound was minimized (38, 39). This novel approach was able to provide configurations with noise signatures that were the closest possible to the target. However, because the procedure was performed on a 1/3-octave band basis and lacked source noise separation of the target sound, the obtained configuration could be inconsistent with the proper source noise mechanism. For example, in one case, high tonal fan noise in the target sound was located within a 1/3-octave band where jet noise has its maximum energy. The optimization process could not distinguish the contribution of the jet noise from the fan noise when they were summed in the same 1/3-octave band, so it raised both components, instead of just the fan, to match the target level in that band. Nevertheless, this effort was one of the first to successfully demonstrate that it is possible to tailor the aircraft design in such a manner to achieve a desired perceptual response. Following the SEFA project, the 2009-13 Community Oriented Solutions to Minimize Aircraft Noise Annoyance (COSMA) (40) continued this type of work, but was directed more toward low-noise operations than to vehicle design (41-43).

4.2 Distributed Electric Propulsion

Electric motors are being considered for use on small aircraft in place of internal combustion engines, and on larger aircraft in place of turbofan engines. Among the many advantages of electric propulsion is the ability to distribute motors in many locations on the vehicle, not just near the power source. This feature has been dubbed distributed electric propulsion (DEP) (44). DEP opens up new degrees-of-freedom in aircraft design, including aerodynamics, vehicle control, and acoustics, to name a few. There are several DEP aircraft in various stages of design and development. A DEP concept, called Leading Edge Asynchronous Propellers Technology (LEAPTech), has been a recent research focus at NASA. LEAPTech is a high-lift system that utilizes a large number of low-speed propellers mounted upstream of the wing leading edge for lift augmentation during low speed operations, see Figure 3. During cruise, the high-lift propellers are folded against their nacelles. Two cruise propellers provide thrust at cruise. Their placement at the wing tips helps reduce induced drag. The most significant benefit of this design is that it allows the wing to be sized for cruise, where the majority of the flight operation is performed. The high aspect ratio, low planform area wing provides reduced cruise drag and improved ride quality (45). LEAPTech is a key technology for a NASA flight demonstrator project called Scalable Convergent Electric Propulsion Technology Operations Research (SCEPTOR), which will retrofit a Tecnam P2006T aircraft with a new, high aspect ratio wing to demonstrate potential efficiency gains that could be realized through such a configuration. An artist depiction of a SCEPTOR-like aircraft is shown in Figure 4.

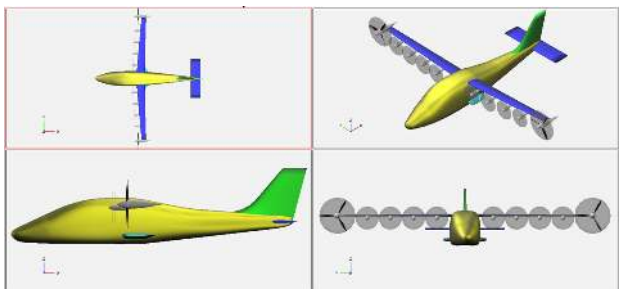

Figure 3 – LEAPTech concept with 8 high-lift propellers (46).

Figure 4 – Artist depiction of SCEPTOR-like aircraft with high-lift system active (47).

4.2.1 Analysis and Design Methodology

The selection of the high-lift propeller system configuration for the SCEPTOR demonstrator is of great importance (47). Fundamental to that is a determination of the number of propellers; a larger number of small propellers versus a smaller number of larger propellers. This, and the manner in which the system operates, affect many performance measures, including acoustics.

A series of high-lift propeller designs were made using the open-source propeller analysis and design tool XROTOR (48). The diameters of the high-lift propellers were determined by the fixed wing span and the number of propellers (NP). A different propeller design was derived depending on propeller diameter. Additionally, for each number of propeller configuration, three-, five-, and seven-blade designs were considered (47). Only the five-blade designs derived from XROTOR served as the basis for this PID effort.

The propellers were designed to have a low tip-speed in an effort to minimize the total radiated sound power, which is proportional to the fifth power of the tip speed (49). Because of solidity considerations, which affect the ability of the propellers to fold against their nacelles, a tip-speed of 137 m/s was maintained across all designs considered. Consequently, the blade passage frequency increased as the diameter decreased. The LEAPTech architecture allows for a change in propeller RPM of up to ± 5% off nominal, without significantly impacting performance. The intentional application of a frequency step (DF) between propellers is referred to as a spread-frequency design, and can significantly alter the sound quality under certain conditions. Spread-frequency designs were explored to determine how annoyance might be affected beyond what might be inferred on the basis of the applicable certification metric L_{Amax}. Note that although the total radiated sound power is largely unaffected by a spread-frequency design, the sound heard by an observer on the ground is affected.

The prediction of noise generated by the high-lift system is not trivial. In addition to both broadband and tonal propeller source noise, there are numerous installation effects including propeller-propeller, propeller-nacelle, and propeller-wing interactions, and other noise sources including electric motor and airframe noise, and wingtip cruise propeller noise. In this exploratory effort, only the tonal component of isolated propeller source noise was included so that early guidance on a spread-frequency design strategy might be provided in the absence of a validated annoyance model. Therefore, the LEAPTech system noise was simulated as a superposition of NP of these components. Efforts are underway, however, to incorporate the broadband component and interaction effects, through a computational fluid dynamics (CFD) approach, to allow higher fidelity simulations in the future.

The propeller noise prediction process is depicted in Figure 5. The propeller description from XROTOR served as input to the Propeller Analysis System (PAS) module (50) of ANOPP, which provided the propeller blade surface pressures. Using Farassat formulation F1A (51) in ANOPP2, the radiated pressure on a hemisphere of discrete points was predicted, from which the pressure time history was synthesized for a time-varying emission angle (46). When CFD results are later available, formulation F1A will again be used as a basis for the synthesis, as indicated in the lower portion of Figure 5.

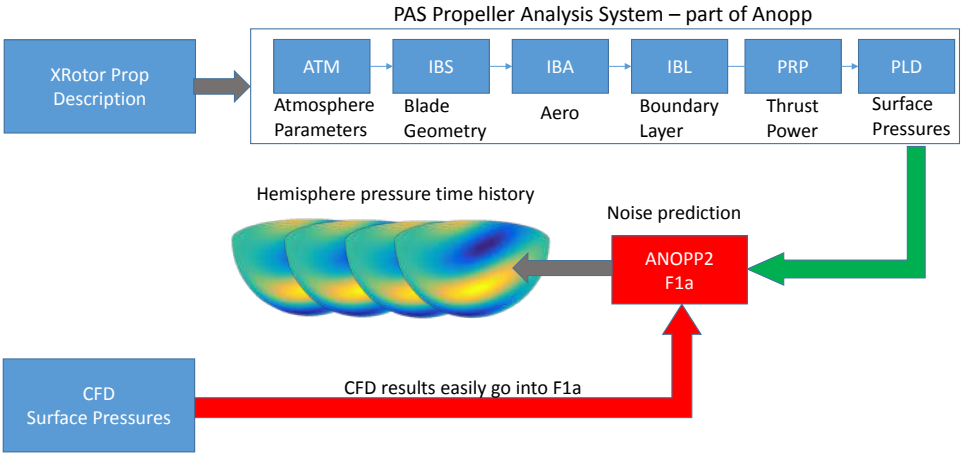

Figure 5 – Propeller noise prediction process (46).

Under 'ideal' operating conditions, Palumbo et al. (46) demonstrated that the synthesized pressure at a ground observer contained very intense fluctuations for spread-frequency ($DF \neq 0$) designs. The intense fluctuations were due to interference of the steady tonal noise generated by multiple propellers. This is unlikely to occur in practice due to physical variances inherent in the electric motor controllers and in the propagation path. Other operating conditions were therefore additionally considered: a 'realistic' condition that contained tight motor control (within 0.1% of set-point) and atmospheric turbulence; a 'randomDF' condition that also had tight motor control and atmospheric turbulence, but with a random spatial distribution of non-integer DF up to the maximum specified; and a 'loose control' condition that was like the 'realistic' condition, but with a larger (1%) motor controller error. In all cases, the spatial distribution of spread-frequency designs was a mirror image between the port and starboard sides of the vehicle. Except for the 'randomDF' condition, the nominal RPM condition was specified at the midspan and the highest RPM located inboard. Flyover sounds for a straight and level trajectory at an altitude of 300 m and flight speed of 31 m/s were generated for each of the above operating conditions. Examples of the flyover sounds generated for DF = 1 Hz are shown in Figure 6 – Figure 9, and are available for download (52). It is seen that the temporal characteristics between sounds vary markedly.

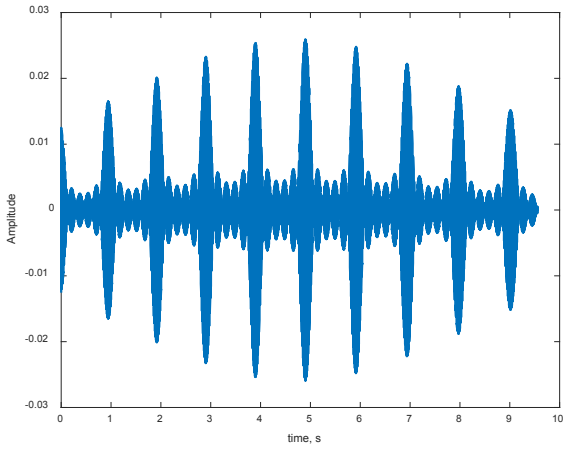

Figure 6 – 'Ideal' operating condition with DF = 1 Hz (46).

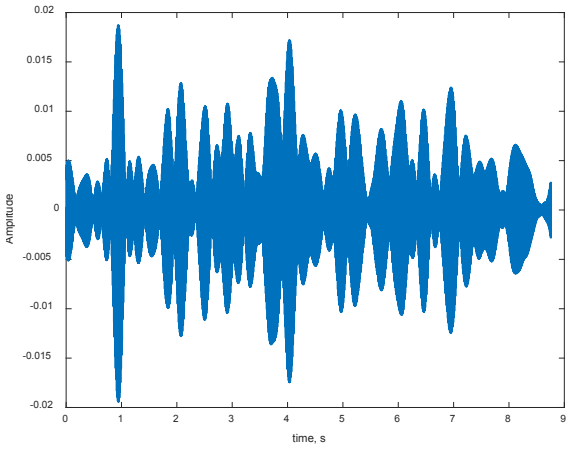

Figure 7 – 'Realistic' operating condition with DF = 1 Hz (46).

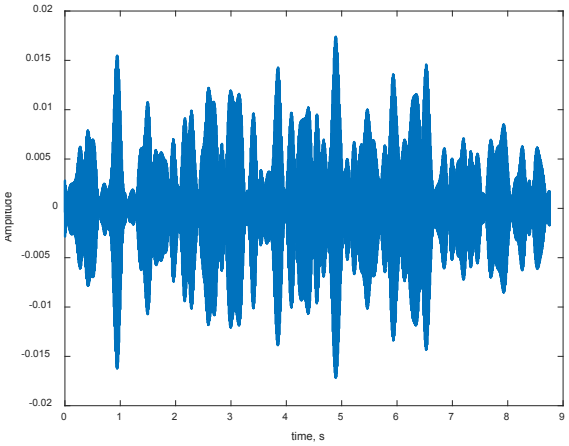

Figure 8 – 'Loose control' operating condition with DF = 1 Hz (46).

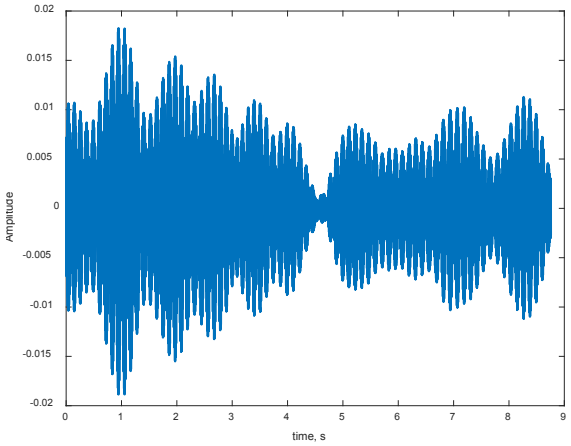

Figure 9 – 'RandomDF' operating condition with a maximum DF = 1 Hz (46).

4.2.2 DEP Psychoacoustic Test

A psychoacoustic test was performed in the Exterior Effects Room (EER) (53) at the NASA Langley Research Center to 1) determine the annoyance associated with different LEAPTech designs as a direct feedback to the design (46), and 2) serve as a basis for annoyance model development (54). The basic dimensions of the test matrix explored NP (6, 12 and 18), and DF (0, 1, 3, 5 Hz). The

blade-passage-frequencies were 161, 332 and 483 Hz for NP of 6, 12, and 18, respectively. Thirty-two subjects rated sounds individually on a continuous rating scale with extreme values of "Not At All" to "Extremely" annoyed, after having been familiarized with the type of sounds included in the test. The test stimuli were 6 s in duration and taken about the overhead position. A brief summary of test findings is next presented.

Annoyance ratings and their 90% confidence intervals are shown in Figure 10 for the 'realistic' operating condition, where "Not At All" annoyed corresponds to a value of 0, and "Extremely" annoyed to a value of 1. The annoyance ratings follow the trends indicated in the L_{Amax} certification metric, shown in Figure 11, confirming that subjects' ratings are based largely on loudness. Annoyance ratings do not follow the trend in unweighted levels, e.g., 54, 50, and 57 dB at DF = 0 for NP = 6, 12 and 18, respectively.

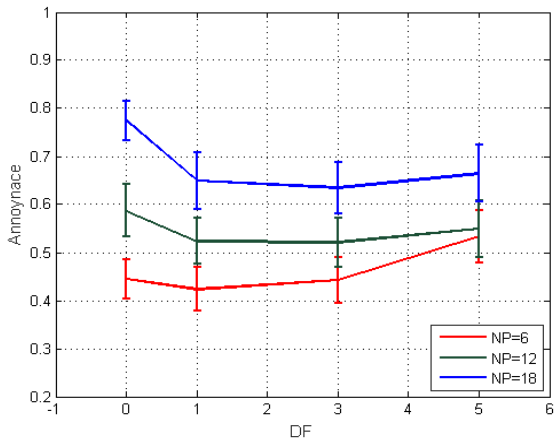

Figure 10 – Mean annoyance as a function of DF & NP under 'realistic' condition (46).

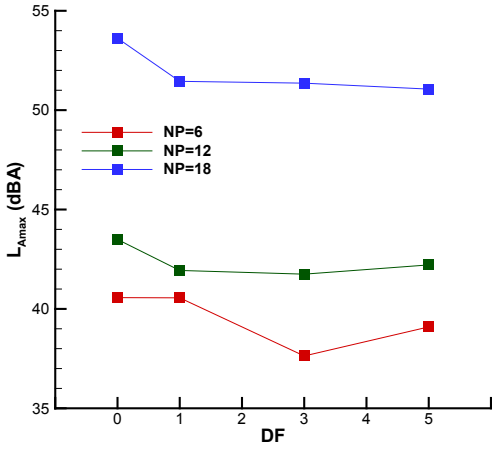

Figure 11 – L_{Amax} as a function of DF & NP under 'realistic' operating condition.

If there were no additional design considerations, the recommendation would be to employ a 6-propeller (NP=6) design with a spread-frequency of 1 Hz. This, however, is not the case. There are other sound types associated with 'loose control' and 'randomDF' conditions. Moreover, there are other factors outside of acoustics that drive the design. Many of these factors drive the design to higher NP (47). One of these is performance related, that is, the total power required, which directly affects range. Figure 12 indicates there is a minimum power requirement at NP=12. Another factor is safety related. Figure 13 shows that a fewer number of propellers raises the one motor out stall speed (above the design stall speed of 55 KEAS) more than does a higher number of propellers. This means that an aircraft with a fewer number of propellers has to fly at a higher flight speed in order to maintain the same margin above stall.

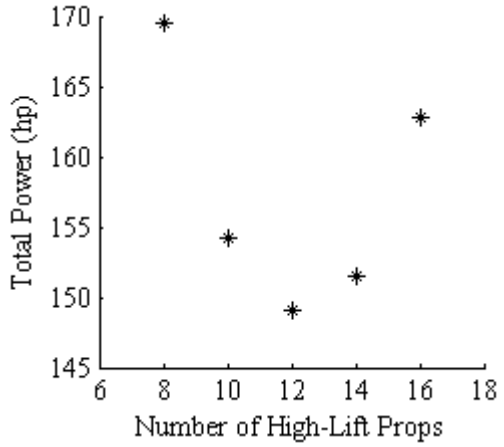

Figure 12 – Total power required as a function of NP (47).

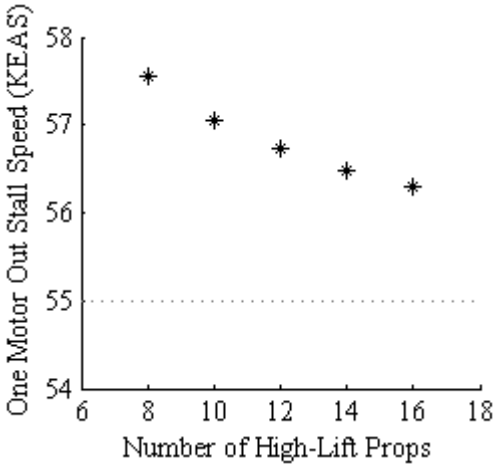

Figure 13 – Stall speed with critical motor inoperative as a function of NP (47).

Shown in Figure 14 are annoyance ratings for NP=12. The 'ideal' condition is the most annoying across DF with a peak at DF=3. Annoyance ratings for non-ideal conditions are more difficult to interpret. Preliminary work in evaluating a multi-parameter annoyance model and developing a new time-varying annoyance model applicable to these types of sounds indicate that loudness accounts for 83% of the variance in annoyance (54). Loudness exceeded 5% of the time, N_5, is shown in Figure 15. The plot of the certification metric L_{Amax}, not shown, looks very similar. As seen by the 'ideal' condition, loudness alone does not fully explain the differences in annoyance between operating conditions. When fluctuation strength and prominence ratio were included, both models accounted for 88% of the variance in annoyance. The fluctuation strength exceeded 5% of the time, FS_5, is shown in Figure 16, and resembles the tent-like distribution in annoyance with DF for the 'ideal' case. Fluctuation strength is greatly diminished for the non-ideal conditions, and consequently, its significance in practical applications may not be as great as indicated here. In the absence of broadband noise components, tonal prominence values, provided in terms of the tone-to-noise ratio (TNR), are exceedingly high, see Figure 17. According to the ECMA-74 standard (55), tones are considered prominent if their TNR is > 8 dB. Below 1 kHz, the threshold of prominence is increased by 2.5 dB/octave. The 'randomDF' and 'loose control' operating conditions are seen to significantly reduce the peak TNR with increasing DF, while a high TNR is maintained across DF for the 'ideal' and 'realistic' conditions.

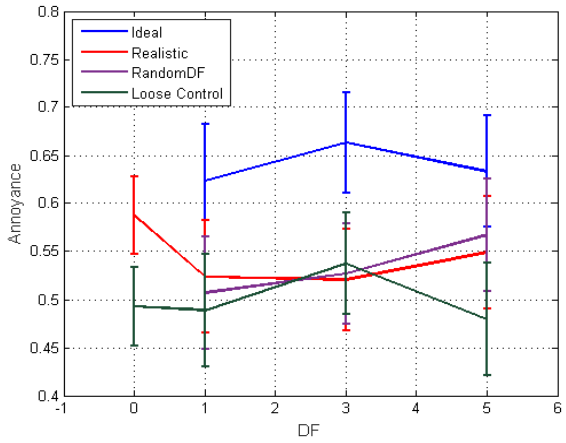

Figure 14 – Mean annoyance as a function of DF & operating condition for NP=12 (46).

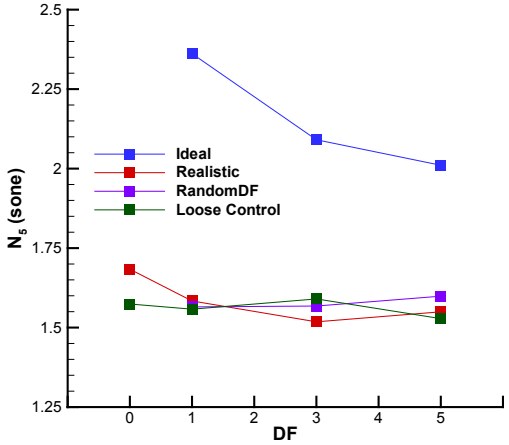

Figure 15 – N_5 loudness as a function of DF & operating condition for NP=12.

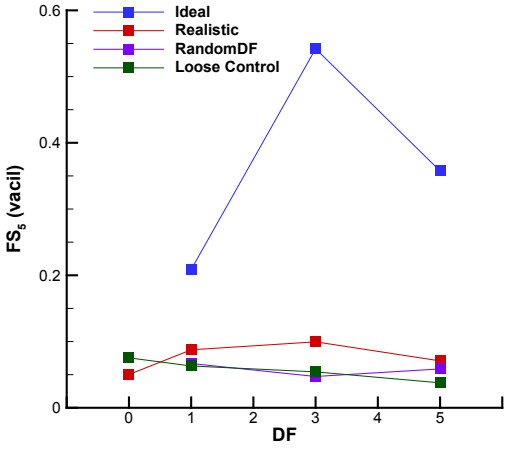

Figure 16 – FS_5 as a function of DF & operating condition for NP=12.

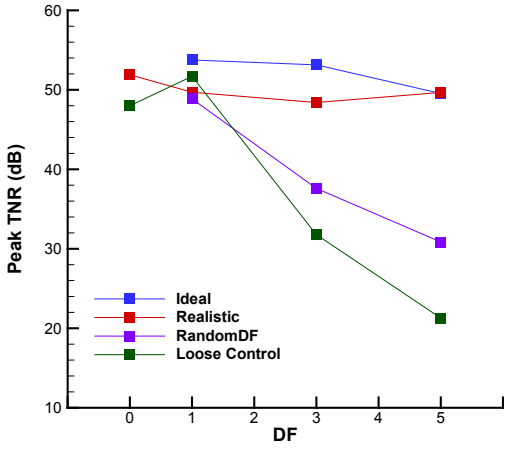

Figure 17 – Peak TNR as a function of DF & operating condition for NP=12.

The insight gained from these models aids in understanding the relationship between annoyance and DEP physical design attributes. Counter to intuition, the data suggests that loose motor control, which presumably comes at a lesser expense than tight motor control, is preferred over the other operating conditions.

4.3 Hybrid Wing Body

The Hybrid Wing Body is an unconventional aircraft configuration that deviates from the traditional tube-and-wing configuration by the installation of engines on top of a lifting body airframe. This configuration offers unique advantages in terms of community noise as the airframe body partially shields engine noise from the ground and airframe noise is reduced through the elimination of high-lift flap systems. NASA started working on low noise HWB concepts in 2001, as a result of aggressive noise goals associated with the QAT project (13). A subsequent NASA-funded conceptual study at the Massachusetts Institute of Technology (MIT) (56) had the objectives of investigating the requirements for an aircraft to be functionally silent, i.e., one with noise below the background noise of a typical well-populated environment, assessing the potential of selected low-noise technologies required for such an aircraft, and conceptualizing aircraft configurations and propulsion airframe integration. In a separate, but related, study funded by the UK government, the Silent Aircraft Initiative (57), Cambridge University partnered with MIT to develop a conceptual design that would have noise imperceptible to the human ear on takeoff and landing in a well-populated area. Both of the earlier MIT and Silent Aircraft Initiative studies identified a large array of advanced technologies and operational changes that would be needed to achieve this aggressive noise goal.

From 2003-05, NASA conducted a pathfinding study to gain a basic understanding of the differences in PAA effects between tube-and-wing and HWB configurations. It also aimed to determine what level of noise reduction might be achievable with a 20-year horizon, along with technologies that might be developed in that timeframe. This study was limited by the almost complete lack of high quality acoustic data or prediction methods for many of the components and, significantly, for the PAA effects, a common situation in that time period. It assessed the potential cumulative (approach + lateral + cutback) noise reduction at 42 EPNdB below the Chapter 4 noise certification requirement (58, 59). This level of noise reduction was clearly aggressive and represented a step change in aircraft noise reduction. It served as the basis for the noise goal of the NASA Environmentally Responsible Aviation (ERA) project. A rendering of one of the final HWB configurations considered under the ERA project and the subject of this case study, a 301-passenger version with two geared turbofan (GTF) like engines, is shown in Figure 18.

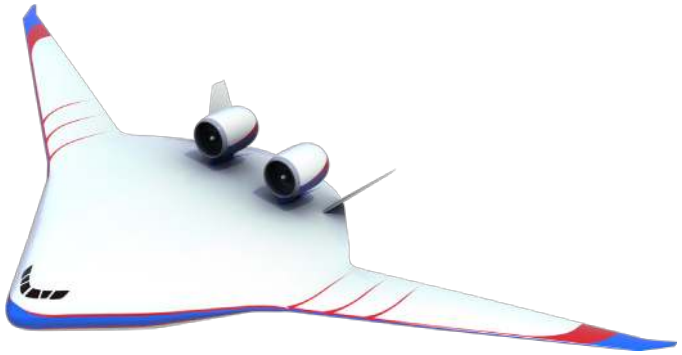

Figure 18 – Rendering of 301-passenger HWB aircraft with GTF-like engines.

4.3.1 Low-Noise Design of HWB Aircraft Concepts under ERA

Since its inception in 2009, the ERA project focused on developing and demonstrating selected technologies for integrated aircraft systems that could meet simultaneously aggressive goals for fuel burn, noise, and emissions (60). The fuel burn goal is for a reduction of 50% relative to a best-in-class aircraft in 2005; the noise goal is 42 EPNdB cumulative below Chapter 4 requirements; and the emissions goal is for a reduction of 75% in NOx below the ICAO Committee on Aviation Environmental Protection (CAEP) 6 standard. The target date is 2020 for key technologies to be at a technology readiness level (TRL) of 4-6 (system or subsystem prototype demonstrated in a relevant environment). This timeline corresponds to a projected aircraft entry into service of 2025. These goals with the timeframe are defined by NASA with the term N+2.

The 301-passenger HWB was one of several advanced aircraft concepts in the large twin aisle (LTA) class studied in the ERA project. It was designed for a 13890 km (7500 nautical mile) mission equivalent to the reference aircraft, a NASA model of the Boeing 777-200LR. An excellent account of the progression in the HWB aircraft conceptual design and noise assessment process, over the course of the ERA Phase I (2009-12) and Phase II (2012-15), is given by Thomas et al. (61). A very brief summary follows.

The fidelity of the conceptual design evolved over the course of the project. From the noise perspective, this was made possible through 1) improvements to system noise prediction models and processes, including the use of extensive integrated system level experimental data for source noise and PAA effects, and 2) design changes including development and integration of noise reduction technologies and takeoff and landing flight path modeling. Another very important aspect was that the design required a multidisciplinary approach in order to simultaneously meet the fuel burn, noise and emissions goals.

The objectives of the next pathfinding study were to initiate the development of higher fidelity data sets including flow and shielding effects needed for the examination of configuration-dependent PAA integration impacts of a HWB concept, start the development of key noise reduction technologies needed to achieve the N+2 goal, and perform a more rigorous system noise assessment than was previously possible. One of the more difficult aspects was jet noise shielding. The system noise assessment (62) was performed using ANOPP and was based upon the 2009 configuration developed by Nickol and McCullers (63), which assumed a technology level consistent with an (earlier) 2020 entry-into-service date. Essential to that effort was an evaluation of the upstream engine placement relative to the trailing edge, exploiting PAA effects of the pylon and chevrons to axially and azimuthally redistribute the noise sources to enhance shielding by the airframe. This was made possible by a high-quality experimental PAA dataset acquired under forward-flight conditions (64). From this dataset, high-fidelity suppression functions were developed for the jet noise source, with lower-fidelity suppression for the fan and core noise, particularly for the tonal components. Another factor identified early on was the added noise associated with the HWB main landing gear which, in its deployed position, is subjected to an airstream close to the free stream velocity. By comparison, the main landing gear for the tube-and-wing reference vehicle is subject to about 80-85% of the free stream velocity. As the landing gear noise source scales with the velocity to the fifth power, subsequent efforts were made to better predict and mitigate the main landing gear noise. A progression of configurations was studied, with the best ultimately evaluated at 42.4 EPNdB cumulative noise reduction below Chapter 4.

During the ERA Phase II, annual noise assessments were performed in 2013 (initial), 2014 (updated), 2015 (final) (65), with a delta final assessment in 2016 (61). During this period, the fidelity of the HWB predictions improved through the introduction of a wide range of N+2 engine and airframe technologies developed by a number of Integrated Technology Demonstration (ITD) teams. Ultra-high bypass ratio GTF-like engines replaced the earlier GE-90-like direct-drive engines. These engines included a low pressure ratio fan with short inlet, swept and leaned fan exit stators, a highly loaded high-pressure compressor, and a low NOx combustor. Through improved PAA design processes based on high-fidelity CFD analyses (66), the engine integration now properly accounted for aerodynamic performance. Consequently, the engines were moved closer to the trailing edge (about one diameter upstream instead of two for the GE-90-like engine), impacting the noise shielding benefit of the airframe. Airframe technologies included a lightweight damage-tolerant composite structure, smaller vertical tails enabled by active flow control, and natural laminar flow nacelle and wing using an advanced high-lift system with a Krueger leading edge having treatment to prevent insect and debris accretion. A set of ITD noise reduction technologies, including soft stator vane technology and a partial main gear fairing, were introduced in the design. A multi-degree-of-freedom (MDOF) acoustic liner in the inlet, bypass duct and interstage region was also included. Additional performance related design changes are detailed in refs. (60, 61, 65), with a chronology of key engine, airframe, propulsion airframe integration, acoustic liner technologies, and other design parameters provided in ref. (61).

The Phase II assessments were performed using the multi-fidelity ANOPP2 framework. Engine source modeling was performed using the ANOPP ST2JET jet noise model with angle of attack correction, the ANOPP GECOR core noise model, and processed experimental data (65) in lieu of a fan noise model. Airframe source modeling was performed using a new Guo-LG (67) landing gear prediction method, an ANOPP BAF-Slat model estimate of the Krueger leading edge flap noise (replaced with a new Guo-Krueger method (68) for the 2016 delta assessment), and the ANOPP FNKAFM trailing edge noise model. PAA effects were predicted as detailed in ref. (65), using the best available experimental data (69-71) from tests conducted at the Boeing Low Speed Aeroacoustics Facility and the NASA Langley 14x22 wind tunnel. Vehicle and engine modeling tools, discussed further in ref. (60), include the NASA Flight Optimization System (FLOPS) (72), Modified Vortex Latice (MVL) (73), Numerical Propulsion System Simulation (NPSS) (74), and Weight Analysis of

Gas Turbine Engines (WATE++) (75). A diagram of the process used for the final 2015 noise assessment is shown in Figure 19.

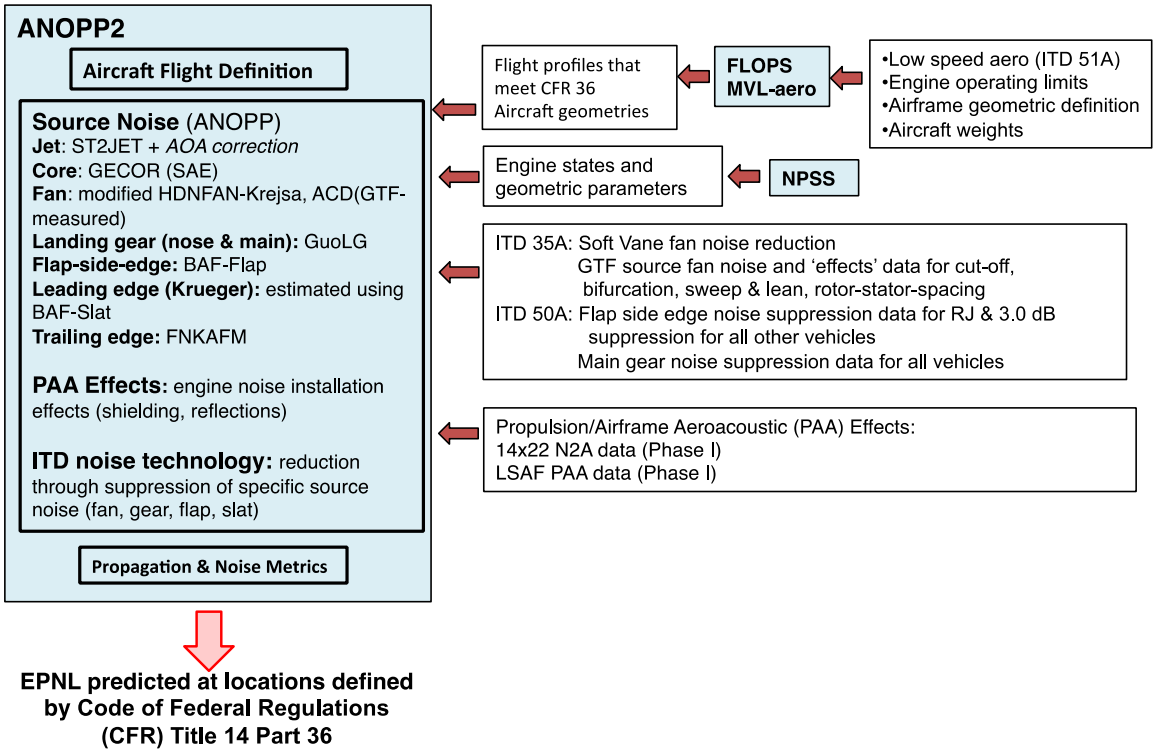

Figure 19 – Overview of the process used for the final 2015 ERA noise assessments (65).

The PNLT traces for the modeled noise components of the HWB301-GTF with ITD noise reduction on approach and sideline are shown in shown in Figure 20 and Figure 21, respectively. These reflect the engine and airframe source noise rankings used at the time of the 2015 final assessments. From these plots, it is clear that the main gear and Krueger flap noise are dominant on approach, while the fan, including PAA effects, is dominant on sideline. When the cutback condition (not shown) is added, the cumulative reduction of 40.3 EPNdB below Chapter 4 nearly achieves the ERA noise goal. Simultaneously, the vehicle exceeded the emissions goal and came close to the fuel burn goal (47% vs the 50% reduction goal), see ref. (60). In the 2016 delta final noise assessment, an adjustment was made to the engine source rankings, yielding nearly the same cumulative reduction of 40.2 EPNdB, but with more substantial changes at the three certification points (61).

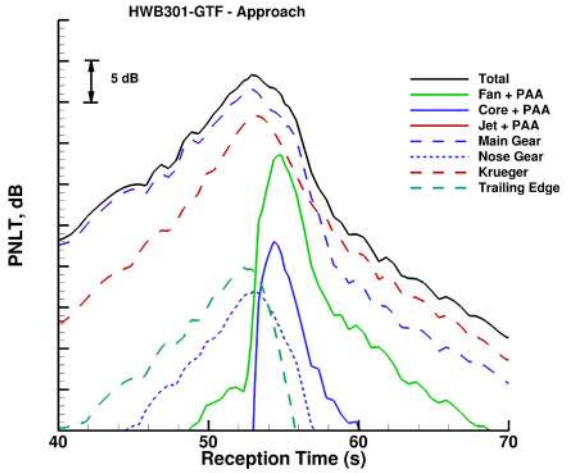

Figure 20 – Noise components and total PNLT for HWB301-GTF on approach (65).

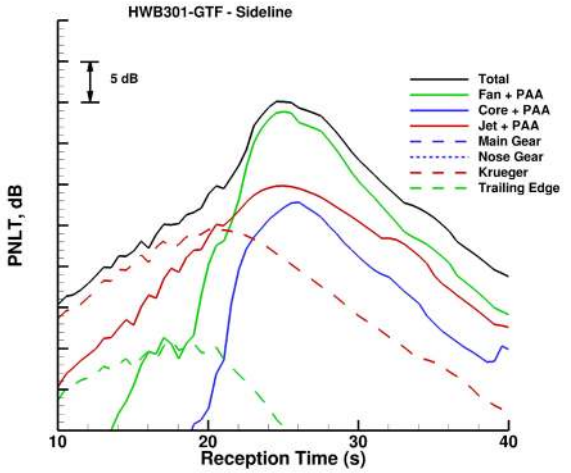

Figure 21 – Noise components and total PNLT for HWB301-GTF on sideline (65)

4.3.2 Psychoacoustic Test of HWB Aircraft Noise

The HWB configuration and its advanced aircraft technologies substantially differs from the tube-and-wing designs constituting the current fleet. The question therefore arises: How well do the PNLT and EPNL metrics, based on psychoacoustic studies conducted in the 1960s and '70s using measured noise from tube-and-wing designs with low bypass ratio turbofan engines, reflect the human annoyance of the HWB. A psychoacoustic test was designed, using auralizations of the LTA reference aircraft and the HWB301-GTF aircraft, to answer the following questions:

1) Are there significant differences in annoyance ratings of sounds taken from similar points in the flyover of different vehicles when presented at the same PNLT level? In other words, is there a significant component of annoyance present in the auralizations that is not captured by PNLT?
2) If so, is there a way to quantify these differences?
3) Can differences in PNLT be used to estimate a change in EPNL between the standard metric value and perceived value?

The auralizations were generated under conditions similar to those used in the 2015 final assessments. The process is detailed in ref. (27), and follows the approach used for auralizing the first ERA noise assessments (31), with an adaptation of the method developed for open rotor noise synthesis (32) applied to the synthesis of GTF fan noise. Pseudo-recordings at locations flush with the ground, for approach and sideline conditions, served as the basis for test stimuli. In all cases, PNLT and EPNL metrics computed from the pseudo-recordings were in very close agreement with those obtained from the system noise predictions under the same conditions (27). Spectrograms of the LTA reference aircraft and HWB301-GTF with ITD noise reduction are shown in Figure 22 at a 1.2 m. high microphone location.

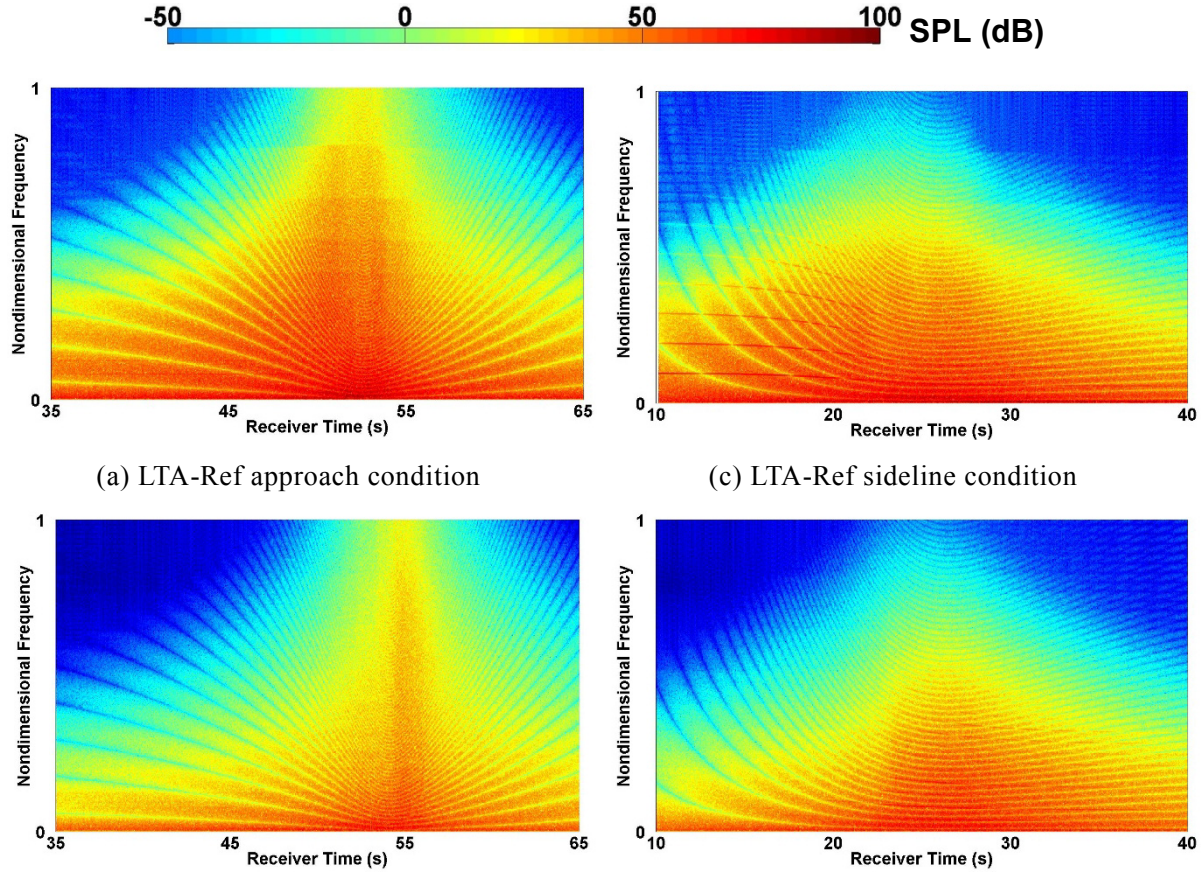

(a) LTA-Ref approach condition

(c) LTA-Ref sideline condition

(b) HWB301-GTF-ITD approach condition

(d) HWB301-GTF-ITD sideline condition

Figure 22 – Spectrograms of auralized flyover noise for LTA class aircraft on approach (a-b) and sideline (c-d) conditions (27). A large dynamic SPL range was used to aid visualization.

The reductions of EPNL between the LTA reference and HWB301-GTF on approach (15.0 EPNdB) and on sideline (7.6 EPNdB) are clearly apparent. Fan tones are clearly visible in the LTA reference vehicle on sideline (c) and to a lesser degree on approach (a), but not at all apparent in the HWB301-

GTF under either condition. Finally, PAA shielding effects are seen to shorten the duration of the high amplitude portion of the HWB301-GTF spectrogram relative to that of the LTA reference. Monaural pseudo-recordings coupled with animations are available for download (52).

The psychoacoustic test was subsequently conducted in the EER at the NASA Langley Research Center. The test and its findings are summarized here; details are found in ref. (76). Short duration signals were extracted from the pseudo-recordings at three points for each approach and sideline condition: the maximum PNLT value, and at both -10 PNdB points defining the interval *d* in eqn. (2). At each extraction point, the signals from the reference and HWB aircraft were presented in pairs (A-B) at equal PNLT levels and subjects were asked to choose which was more annoying. In 4 of the 6 comparisons, subjects found one signal more annoying than the other (with $p \leq 0.05$), indicating that something not captured by PNLT is likely causing differences in annoyance.

The differences were then quantified by presenting the signals at different levels relative to each other to determine the level at which the two sounds were equally annoying. Figure 23 demonstrates this for the LTA (A) – HWB (B) pair on approach at the maximum PNLT point, indicating that the HWB (B) signal must be reduced by 2.1 dB to be equally annoying as the LTA (A) signal. With the equal annoyance point defined at the three extraction points, it is possible to estimate the psychoacoustic difference in EPNL between the two signals by estimating the equal annoyance PNLT and recomputing EPNL, as depicted in Figure 24.

From the test data, it was found that the mean difference in EPNL values between the LTA reference and the HWB301-GTF was decreased by 1.24 EPNdB on approach and 2.04 on sideline. To put these numbers into perspective, these are on the order of the 1-2 EPNdB cumulative noise reduction achieved through introduction of the ITD noise reduction technology and multiple degree-of-freedom acoustic duct liners, when their contributions are assessed one-by-one (65). Further studies are needed to determine if the differences are due to an underprediction of annoyance by PNLT and EPNL for the HWB301-GTF, or an overprediction of annoyance of the reference aircraft. The estimated noise reduction obtained in this test trend in the same direction as those obtained with the EPNL metric, but differ significantly in magnitude. This indicates that a low-noise design, as expressed by EPNL reduction, does not necessarily equate with a low-annoyance design. Further, it suggest that a design incorporating more than just EPNL as the noise cost functional is worthy of consideration. It may, for example, be worthwhile to consider a psychoacoustic metric that explicitly accounts for tonal amplitude and spectral distribution as a means of influencing the design, as some of the sounds had high TNRs, see ref. (76). The tone penalty used in the PNLT calculation, after all, is based upon relative levels of adjacent 1/3-octave bands, not on the tonal amplitudes themselves.

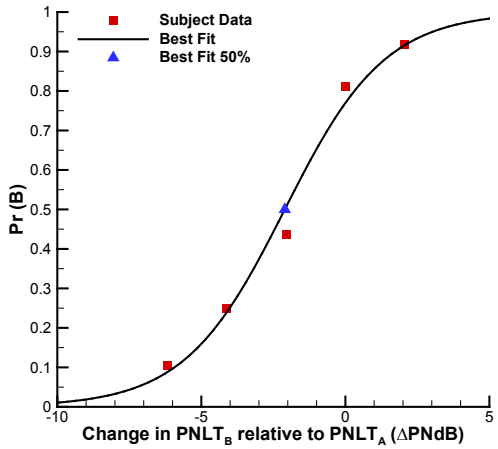

Figure 23 – Fit of response data for HWB301-GTF (B) rel. to LTA ref (A) on approach.

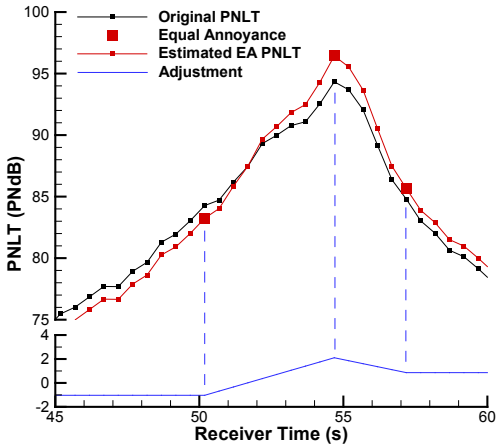

Figure 24 – PNLT adjustment of HWB301-GTF rel. to LTA reference on approach (76).

4.4 Low-Boom Supersonic Aircraft

There is considerable international interest in development of a commercial low-boom supersonic aircraft. The current ban on supersonic commercial flight over land is due, in large part, to the high levels of annoyance associated with far-field N-wave shaped sonic booms associated with supersonic cruise. The transition focus boom as the aircraft accelerates from subsonic to supersonic speeds is also a concern. Sonic boom is not just an issue on the aircraft ground track. The region of the

primary and secondary boom can extend tens of kilometers in width, see Figure 25, and is a factor that must be taken into account for an effective low-boom design.

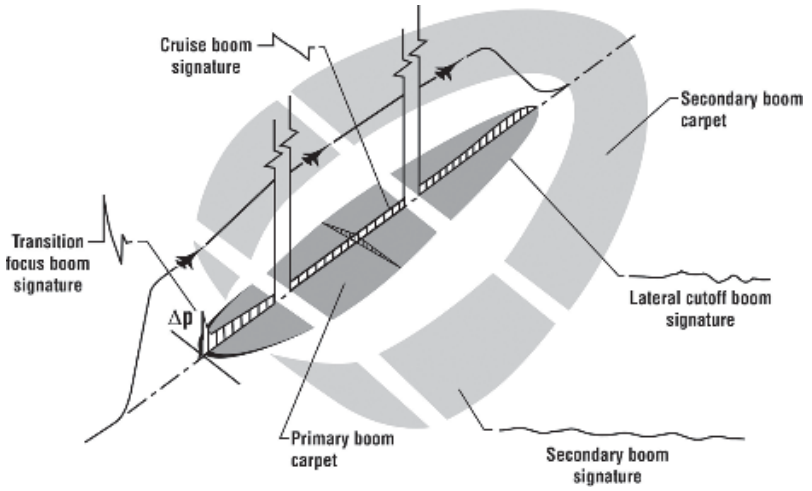

Figure 25 – Schematic of sonic boom ground exposure (77).

It has been known since the mid-1960s that sonic booms can propagate to the ground without ever reaching the far-field (78). These midfield booms have reduced overpressure and rise time compared to far-field booms depicted in Figure 25 at cruise. Midfield booms result from atmospheric absorption countering the steepening of the waveform due to nonlinear effects. Consequently, sound propagation effects take on a more significant role in the design of low-boom aircraft than they do for airport community noise. Much of the development of low-boom technology has been based on the idea of shaping the aircraft in a way that does not allow an N-wave shaped boom to evolve and reach the ground. An excellent overview of the influence of the atmosphere and techniques for boom minimization through aircraft shaping can be found in chapters 2 and 5 of ref. (77), respectively.

4.4.1 Sonic Boom Analysis

The foundations for sonic boom theory were established by Whitham (79, 80) and Walkden (81), who described the near-field overpressure, δp, distribution as

$$\delta p(\chi,\theta) = \frac{p_a \gamma M^2}{\sqrt{2\beta r}} F(\chi,\theta) \tag{3}$$

in which M is the Mach number, p_a is the ambient pressure, γ is the ratio of specific heat, β is the Prandtl–Glauert factor ($\sqrt{M^2-1}$), r and x are perpendicular and parallel to the flight path, respectively, and lines of constant $\chi = x - \beta r$ are perpendicular to the propagation path. The "F-function" is given by

$$F(x,\theta) = \frac{1}{2\pi}\int_0^x \frac{A_v''(\bar{x},\theta) + \beta/2q_\infty L'(\bar{x},\theta)}{\sqrt{x-\bar{x}}}\, d\bar{x} \tag{4}$$

in which A_v'' is the volume contribution expressed in terms of the second derivative of the longitudinal area distribution, and is determined by cross sections measured across cutting planes aligned with the Mach angle, that is, along $\bar{x}$. The term L' is the first derivative of the lift distribution, also taken along the Mach cutting planes, and q_∞ is the free stream dynamic pressure. The numerator of the integral in eqn. (4), taken before differentiation, is referred to as the effective area and is given by

$$A_e(\bar{x},\theta) = A_v(\bar{x},\theta) + \frac{\beta}{2q_\infty}\int_o^x L(\bar{x},\theta)\, d\bar{x} \tag{5}$$

Note that eqn. (3) is referred to as near-field because the distribution (shape) changes with distance due to nonlinear effects. It is, however, a far-field radiating solution.

By ensuring A_e to be a smooth function of length, the F-function and consequently the near-field pressure distribution are minimized. A low-boom design thus requires: a smooth volume distribution, taking into account detailed features of the outer mold line (OML) from nose to tail, such as engine installation; and a smooth lift distribution provided by highly swept wings designed for high speed

aerodynamic performance at cruise. Seebass and George subsequently provided the theoretical basis for aerodynamic minimization of the sonic boom with analytic forms of the F-function (82, 83). These days, use of analytic F-functions for minimization of sonic booms has been largely superseded by CFD (84). However, because far-field solutions from CFD are computationally prohibitive, alternative methods were developed to bridge the gap, e.g., obtaining the near-field CFD solution for δp on a cylinder about the vehicle (85), then reconstituting the far-field radiating solution by the method of George (86).

With the far-field radiating solution in hand, the sonic boom may be propagated to the ground through geometrical ray tracing, taking into account nonlinearity, atmospheric absorption, and spreading. Several computer codes are available for doing so, e.g., PCBoom (87) and sBOOM (88). An excellent, albeit somewhat dated, summary of sonic boom modeling is given by Plotkin (89).

Flight Test Validation

In 2003 and 2004, the United States Defense Advanced Research Projects Agency (DARPA) Shaped Sonic Boom Demonstration (SSBD) Program and the NASA Shaped Sonic Boom Experiment (SSBE) conducted a number of flight tests to validate CFD and propagation analyses that indicated it was possible to generate a sonic boom with a tailored flat-top signature at the ground. Results from near-field CFD analyses, like that shown in Figure 26, were used to design modifications to the OML at the front of a Northrop Grumman F-5E to produce a strong bow shock with a relatively flat pressure distribution back to the engine inlet. The modified aircraft used in the flight tests is shown in Figure 27. Near-field pressure measurements, taken in-flight by an instrumented F-15B aircraft flying beneath and aft of the test aircraft, are compared with near-field CFD results in Figure 28. The F-15B flight path is depicted by the dark trace in Figure 26. The resulting boom signature at the ground relative to the baseline F-5E N-wave boom is shown in Figure 29. The excellent comparison of the near-field pressures in Figure 28 and flat-top shape in Figure 29 serve to validate the tool chain.

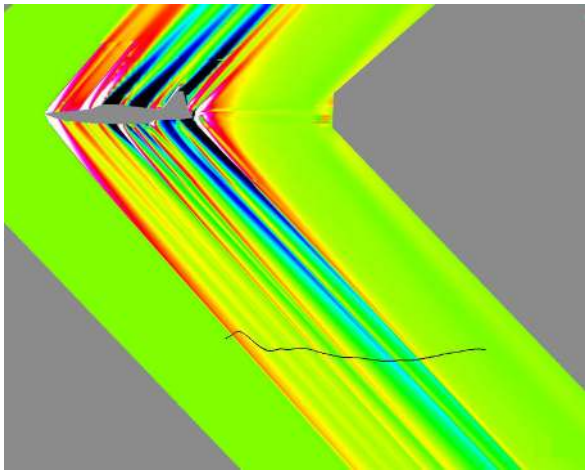

Figure 26 – CFD-computed near-field pressure of modified F-5E (90).

Figure 27 – Photograph of modified F-5E used in SSBD and SSBE flight tests (91).

4.4.2 Psychoacoustic Tests

Considerable effort has gone into understanding human response to sonic boom, see chapter 8 in ref. (77), in an effort to determine metric(s), which can be used for design and which might serve as a scientific basis for possible future regulations permitting supersonic flight over land.

A series of laboratory studies were conducted in the sonic boom simulator (92) at the NASA Langley Research Center in the early 1990s to quantify loudness and annoyance response to a wide range of shaped sonic boom signatures. Summary findings are presented in ref. (93).

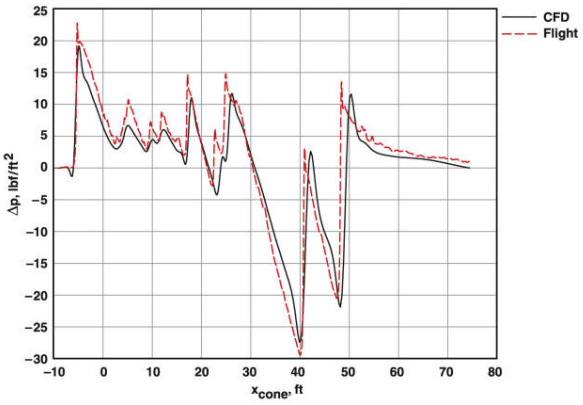

Figure 28 – Comparison of near-field CFD and flight measurements (90).

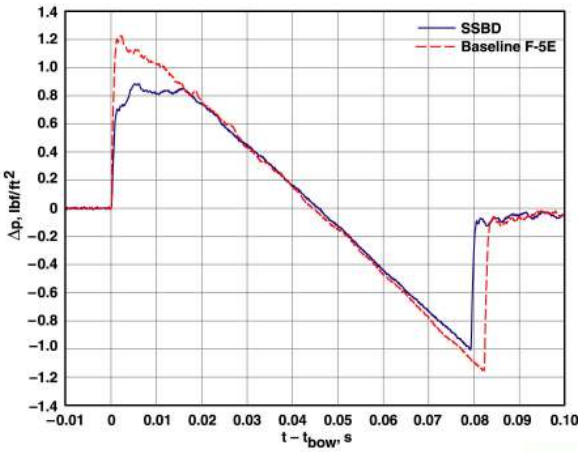

Figure 29 – Comparison of modified SSBD and baseline booms at the ground (90).

Shepherd and Sullivan (10) showed that the PL of N-waves is controlled by the overpressure and associated rise time. In contrast, the PL of shaped booms is dependent on characteristics of the initial and aft shocks, and subtleties of the waveform shape. Consequently, the PL of shaped booms could be significantly less than the PL of N-waves having the same peak overpressure. A psychoacoustic test (94) was performed to determine if this was reflected in subjective loudness ratings. The results indicated that front-shock-minimized (FSM) booms were rated quieter than N-waves with comparable peak overpressures. For a given subjective loudness rating, the FSM waveforms (except for flat-top waveforms) had much higher peak overpressures than the N-waves. This result suggests that supersonic aircraft designed to minimize sonic booms, i.e., to have a lower PL, should have lower subjective loudness ratings and therefore be more acceptable than those not designed in this manner. Other studies discussed in ref. (93) further support the idea of using PL as a design metric. In one of those studies, composite (direct plus simulated ground-reflected) N-waves and FSM waveforms were presented. There, PL was found to correlate the highest with subjective loudness ratings.

Differences in response ratings between outdoor and indoor conditions were also studied using unfiltered (outdoor) and filtered (indoor) N-waves and FSM waveforms. Two indoor conditions were considered, representing transmission into a residential structure with and without the windows open. For both outdoor and indoor booms, the preferred subjective response estimator describing loudness and annoyance was PL. For outdoor booms, there was no significant difference in mean loudness and annoyance ratings. For indoor booms, however, there was a difference, with annoyance registering higher mean values than loudness for both windows-open and windows-closed conditions. This means people indoors respond to factors beyond loudness when making annoyance judgments. The subjective benefit derived from minimizing the boom shape was accounted for by PL for both outdoor and indoor environments.

The topic of indoor versus outdoor annoyance to sonic boom is an area of active research. Recent psychoacoustic tests in the Interior Effects Room (IER) (95) at the NASA Langley Research Center and at other test facilities (96, 97) were aimed at understanding these differences. Earlier findings showing PL as a good indicator of indoor and outdoor annoyance were first reproduced in the IER (98). The effects of rattle were then studied (99-101) indicating that differences in annoyance not accounted for by PL could be accounted for when PL was modified by the difference between C-weighted and A-weighed SEL, that is, PL + (L_{CE} -L_{AE}). Additional studies are planned to continue investigation of the effects of rattle and vibration, and their relative importance to overall perception of sonic boom experienced indoors.

4.4.3 PID of Low-Boom Aircraft

PID of low-boom supersonic aircraft concepts has been enabled by incorporation of PL and other psychoacoustic metrics as design constraints within MDAO design processes. An example is the multi-fidelity design and analysis capability that has been built around the ModelCenter software integration framework (102). Any such framework must take into account the mission (range, payload, and speed), low- and high-speed aerodynamic and propulsive performance, structures, etc., in addition to sonic boom acceptability. As an aside, an additional factor in the design of supersonic aircraft is the mitigation of community noise. Because the use of large high-bypass ratio engines

found on subsonic commercial aircraft is not practical due to their high drag at supersonic cruise, smaller low-bypass ratio engines must be used, which increases jet noise. The Chapter 4 or 14 noise certification rules would likely apply to airport community noise of any future commercial supersonic aircraft.

Even more recent developments have focused on adjoint methods, which allow sensitivities of ground-based cost functional(s) with respect to design features to be determined. An example of this can be found by Rallabhandi et al. (103), where sensitivities of the L_{AE}-based cost functional to the aircraft OML were determined. Here, L_{AE} was selected over PL because its calculation method was more amenable to generating the required sensitivities. In Rallabhandi's work, the optimization was broken into two phases. In the "front shaping" phase, the forward fuselage and wing shapes of the baseline geometry were optimized to minimize the cost functional. This baseline geometry itself was the result of earlier optimization efforts. In the "optimum" phase, the aft fuselage and tail sections, in addition to the forward fuselage and wing, were optimized. The optimized near-field pressure waveforms shown in Figure 30 result from shock cancellation through relative placement of shock and expansion regions, and wing shock structure redistribution. Small changes in the aft shock structure are enough to make an additional 1 dBA reduction in the ground signature (on top of the 4.3 dBA reduction from the front shaping phase) relative to the baseline, as seen in Figure 31.

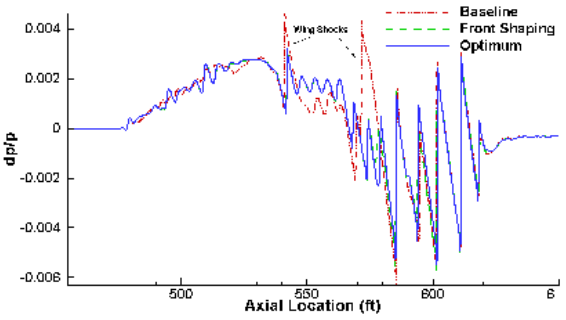

Figure 30 – Baseline and optimized near-field pressure waveforms (103).

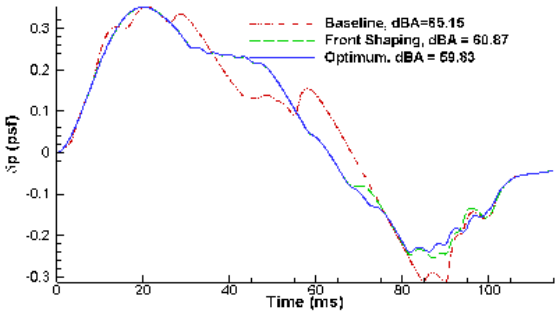

Figure 31 – Comparison of ground signatures (103).

As a result of 1) flight test validated methods for shaping the boom at the ground, 2) an understanding of noise metrics which describe the human response to sonic booms, and 3) an aircraft design capability which can be influenced by that knowledge, NASA recently awarded a contract to the Lockheed Martin Aeronautics Company for the preliminary design of a low-boom flight demonstration aircraft. The Quiet Supersonic Technology (QueSST) X-plane will be designed with a low-boom goal of 75 dB, making it greater than 8 time less loud than the Concorde. In addition to validating design methods for achieving this goal, the QueSST aircraft will be used to collect community response data to assess the relationship between annoyance and noise exposure for real airplanes and real communities. It will also allow investigations of cumulative exposure metrics not possible in the laboratory environment. An artist's depiction of the QueSST X-plane is shown in Figure 32.

5. CONCLUSIONS

This paper puts forth the proposition that it is possible to influence the design of aircraft to simultaneously meet noise certification and other design requirements, and achieve some desirable, or less undesirable, noise attributes that are not reflected in the noise certification metrics. This has been made possible by providing the means for human subject response to act as feedback to the design process, either directly or through the use of metrics, which correlate with human response and which can be used as additional cost functionals in design.

Four case studies were considered to demonstrate the perception-influenced design philosophy using annoyance and loudness as measures of subjective response. The cases selected had more to do with what was accessible to the author than any known limitations of the approach. The most effective use of perception-influenced design is when the noise cost functional used in that design is based on sounds that do not correlate well with the subjective response that one desires to minimize.

Figure 32 – Artist's concept of the low boom flight demonstration QueSST X-plane.

Indeed, there are near-term research plans to apply this capability to two air vehicles, which many people find annoying, yet certify under current regulations. In the first, the effectiveness of low-noise rotor designs developed on the basis of the helicopter L_{AE} certification metric will be assessed for annoyance, with the objective of ultimately influencing the design. In the second, prediction tools and subjective response data needed for design of low-annoyance sUAS, such as those proposed for package delivery, will be explored. While not the focus of this paper, the use of perception-influenced design for development of low noise operations, such as those investigated in the COSMA project, has great future potential, particularly when considering vehicle operations that are not concentrated around an airport. Additionally, the body of knowledge being generated on human response to low-boom aircraft, using prediction-based signatures, will hopefully one day contribute to the selection of a certification metric for supersonic passenger aircraft.

Finally, even though perception-influenced design has been shown to have the potential to influence the design of future aircraft, its widespread use is not expected anytime soon. Indeed, the operative word in the title of this paper is "toward." Minimally, it will take further development of tools and methods, and successful demonstration of the approach on vehicle noise issues that are denying entry into markets, before it is accepted by those directly and indirectly involved in aircraft design. This work is meant to be a step in that direction.

ACKNOWLEDGEMENTS

This work was performed with support from the Transformational Tools and Technologies project and the Convergent Aeronautics Solutions project of the NASA Transformative Aeronautics Concepts Program, the Environmentally Responsible Aviation project of the NASA Integrated Aviation Systems Program, and the Commercial Supersonic Technology project of the NASA Advanced Air Vehicles Program.

The author wishes to thank Karl Janssens (Siemens) and Umberto Iemma (Università Degli Studi Roma Tre) for their consultation on the SEFA/COSMA case study; Dan Palumbo (Structural Acoustics Branch, NASA Langley), Menachem Rafaelof (National Institute of Aerospace), and Michael Patterson (Aeronautics Systems Analysis Branch, NASA Langley) for their assistance on the DEP case study; Casey Burley and Russ Thomas (Aeroacoustics Branch, NASA Langley) for their assistance on the HWB case study; and Alexandra Loubeau and Kevin Shepherd (Structural Acoustics Branch, NASA Langley), Peter Coen (Aeronautics Research Directorate, NASA Langley) and Sriram Rallabhandi (National Institute of Aerospace) for their assistance on the low-boom supersonic aircraft case study.

REFERENCES

1. Miedema HME, Vos H. Exposure-response relationships for transportation noise. Journal of the Acoustical Society of America. 1988;104(6):3432-45.
2. Fields JM. Effect of personal and situational variables on noise annoyance in residential areas. Journal of the Acoustical Society of America. 1993;93(5):2753-63.
3. Annex 16 to the Convention on International Civil Aviation, Environmental Protection, Volume I, Aircraft Noise (7th Edition). International Civil Aviation Organization, Montreal, Canada; 2014. p. 236.
4. Guidance on the balanced approach to aircraft noise management (2nd Edition). International Civil Aviation Organization, Montreal, Canada, 2008, Doc 9829, AN/451.
5. Noise standards: aircraft type and airworthiness certification, CFR Title 14, Chapter 1 - Federal Aviation Administration, Department of Transportation, Part 36 (2016 Edition).
6. Article 6 - Essential requirements for environmental protection, Regulation (EC) No 216/2008 of the European Parliament and of the Council (2008).
7. Heathrow Airport, Airport charges structural review. Heathrow Airport Limited, 2015.
8. Kryter KD. Scaling human reactions to the sound from aircraft. Journal of the Acoustical Society of America. 1959;31(11):1415-29.
9. Bennett RL, Pearsons KS. Handbook of aircraft noise metrics. NASA, 1981 CR 3406.
10. Shepherd KP, Sullivan BM. A loudness calculation procedure applied to shaped sonic booms. NASA, 1991 TP 3134.
11. Stevens SS. Percieved level of noise by Mark VII and decibles (E). Journal of the Acoustical Society of America. 1972;51(2B):575-601.
12. Johnson DR, Robinson DW. The subjective evaluation of sonic bangs. Acustica. 1967;18(5):241-58.
13. Whitfield CE. NASA's Quiet Aircraft Technology Project, Paper ICAS 2004-6.10.1 (I.L.) 24th International Contress of the Aeronautical Sciences (ICAS2004); Yokohama, Japan, 2004.
14. Darecki M, Edelstenne C, Enders T, Fernandez E, Hartman P, Herteman J-P, et al. Flightpath 2050, Europe's vision for aviation. Belgium: European Commission, 2011.
15. NASA aeronautics strategic implementation plan (NP-2015-03-1479-HQ) Washington, DC, : NASA; 2015. Available from: http://www.aeronautics.nasa.gov/strategic-plan.htm.
16. Moore MD, Ken G, Viken J, Smith J, Fredericks B, Trani T, et al. High-speed mobility through on-demand aviation, AIAA-2013-4373. AIAA Aviation Technology, Integration, and Operations Conference; Los Angeles, CA, 2013.
17. Zorumski WE. Aircraft noise prediction program theoretical manual. NASA, 1982 TM-83199.
18. Lopes LV, Burley CL. Design of the next generation aircraft noise prediction program: ANOPP2, AIAA 2011-2854. 17th AIAA/CEAS Aeroacoustics Conference; Portland, OR, 2011.
19. Bertsch L, Isermann U. Noise prediction toolbox used by the DLR aircraft noise working group. InterNoise 2013; Innsbruck, Austria, 2013.
20. LeGriffon I. Aircraft noise modelling and assessment in the IESTA program with focus on engine noise. 22nd International Congress on Sound and Vibration (ICSV22); Florence, Italy, 2015.
21. Davies P. Perception-based engineering: Integrating human responses into product and system design. The Bridge. 2007;37(3):18-24.
22. Lyon RH. Product sound quality – from perception to design. Sound and Vibration. 2003;37(3):18-23.
23. Otto N, Amman S, Eaton C, Lake S. Guidelines for jury evaluations of automotive sounds, SAE Technical Paper 1999-01-1822. Noise and Vibration Conference, 1999.
24. Christian A, Boyd Jr. DD, Zawodny NS, Rizzi SA. Auralization of tonal rotor noise components of a quadcopter flyover. InterNoise 2015; San Francisco, CA, 2015.
25. Rizzi SA. Tools for assessing community noise of DEP vehicles. AHS-AIAA Transformative Vertical Flight Concepts Joint Workshop on Enabling New Flight Concepts through Novel Propulsion and Energy Architectures; Arlington, VA, 2014.
26. Rizzi SA, Christian A. A method for simulation of rotorcraft fly-in noise for human response studies. InterNoise 2015; San Francisco, CA, 2015.
27. Rizzi SA, Burley CL, Thomas RH. Auralization of NASA N+2 aircraft concepts from system noise predictions, AIAA-2016-2906. 22nd AIAA/CEAS Aeroacoustics Conference; May 30 - June 1; Lyon, France, 2016.
28. Berckmans D, Janssens K, Sas P, Desmet W, Van der Auweraer H. A new method for aircraft noise synthesis. International Conference on Noise and Vibration Engineering; September 18-20; Leuvan, Belgium, 2006. p. 4257-70.
29. Sahai A, Anton E, Stumpf E, Wefers F, Vorlaender M. Interdisciplinary auralization of take-off and landing

procedures for subjective assessment in virtual reality environments, AIAA-2012-2077. 18th AIAA/CEAS Aeroacoustics Conference; Colorado Springs, CO, 2012.
30. Arntzen M, D.G. Simons DG. Modeling and Synthesis of Aircraft Flyover Noise. Applied Acoustics. 2014;84:99-106.
31. Rizzi SA, Aumann AR, Lopes LV, Burley CL. Auralization of hybrid wing-body aircraft flyover noise from system noise predictions. AIAA Journal of Aircraft. 2014;51(6):1914-26.
32. Rizzi SA, Stephens DB, Berton JJ, Van Zante DE, Wojno JP, Goerig TW. Auralization of flyover noise from open rotor engines using model scale test data. AIAA Journal of Aircraft. 2016;53(1):117-28.
33. Sahai A, Wefers F, Pick S, Stumpf E, Vorländer M, Kuhlen T. Interactive simulation of aircraft noise in aural and visual virtual environments. Applied Acoustics. 2016;101:24-38.
34. Rietdijk F, Heutschi K, Zellmann C. Determining an empirical emission model for the auralization of jet aircraft. Euronoise 2015; Maastricht, The Netherlands, 2015. p. 781-4.
35. SEFA report summary: European Commission, Community Research and Development Information Service; 2011. Available from: http://cordis.europa.eu/result/rcn/47580_en.html.
36. Bisping R. Aircraft target sound design. 12th International Congress on Sound and Vibration (ICSV12); Lisbon, Portugal, 2005.
37. Janssens K, Vecchio A, Van der Auweraer H. Model-based synthesis approach for vehicle and aicraft noise. Euronoise Conference; Tampere, Finland, 2005.
38. Diez M, Iemma U, Marchese V. A sound-matching-based approach for aircraft noise annoyance alleviation via MDO, AIAA-2007-3667. 13th AIAA/CEAS Aeroacoustics Conference; Rome, Italy, 2007.
39. Diez M, Iemma U. Multidisciplinary conceptual design optimization of aircraft using a sound-matching-based objective function. Engineering Optimization. 2012;44(4):591-612.
40. Bauer M, Collin D, Iemma U, Janssens K, Márki F, Müller U. COSMA - A European approach on aircraft noise annoyance research. InterNoise 2014; Melbourne, Australia, 2014.
41. Iemma U, Diez M, Leotardi C, Centracchio F. Multi-objective, multi-disciplinary optimization of take-off and landing procedures to minimize the environmental impact of commercial aircraft: The noise vs fuel consumption trade-off within the EC project COSMA. 19th International Conference on Sound and Vibration (ICSV19); Vilnius, Lithuania, 2012.
42. Iemma U, Burghignoli L, Centracchio F, Galluzzi V. Multi-objective optimization of takeoff and landing procedures: level abatement vs quality improvement of aircraft noise. InterNoise 2014; Melbourne, Australia, 2014.
43. Iemma U. Multi-disciplinary, community-oriented design of low-noise aircraft: the COSMA project. Noise Mapping. 2016;3(1):59-70.
44. Moore MD, Fredericks WJ. Misconceptions of electric propulsion aircraft and their emergent aviation markets, AIAA 2014-0535. 52nd AIAA Aerospace Sciences Meeting; National Harbor, MD, 2014.
45. Stoll AM, Bevirt J, Moore MD, Fredericks WJ, Borer NK. Drag reduction through distributed electric propulsion, AIAA 2014-2851. 14th AIAA Aviation Technology, Integration, and Operations Conference; Atlanta, GA, 2014.
46. Palumbo D, Rathsam J, Christian A, Rafaelof M. Perceived annoyance to noise produced by a distributed electric propulsion high lift system. Spring 2016 Acoustics Technical Working Group Meeting; Hampton, VA, 2016.
47. Patterson MD, Derlaga JM, Borer NK. High-lift propeller system conguration selection for NASA's SCEPTOR distributed electric propulsion flight demonstrator. 16th AIAA Aviation Technology, Integration, and Operations Conference; Washington, DC, 2016.
48. Drela M, Youngren H. XROTOR Download Page, [cited 2014 26 May]. Available from: http://web.mit.edu/drela/Public/web/xrotor/.
49. AIR 1407, Prediction procedure for near-field and far-field propeller noise. A-21 Committee on Aircraft Noise Measure Noise Aviation Emission Modeling. Warrendale, PA: SAE International; 1977.
50. Nguyen LC, Kelly JJ. A users guide for the NASA ANOPP Propeller Analysis System. NASA, 1977 CR-4768.
51. Farassat F. Derivation of formulations 1 and 1A of Farassat. NASA, 2007 TM-2007-214853.
52. Aircraft flyover simulation: NASA; 2016. Available from: http://stabserv.larc.nasa.gov/flyover/.
53. Faller II KJ, Rizzi SA, Aumann AR. Acoustic performance of a real-time three-dimensional sound-reproduction system. NASA, 2013 TM-2013-218004.
54. Rafaelof M. A model to gauge the annoyance due to arbitrary time-varying sound, Paper 68. NOISE-CON 2016; Providence, RI, 2016.
55. Measurement of airborne noise emitted by information technology and telecommunications equipment. ECMA International, 2008 ECMA-74 10th Edition.

56. Manneville A, Pilczer D, Spakovszky ZS. Preliminary evaluation of noise reduction approaches for a functionally silent aircraft. Journal of Aircraft. 2006;43(3):836-40.
57. Hileman J, Spakovszky ZS, Drela M, Sargeant MA. Airframe design for "silent aircraft", AIAA-2007-453. 45th AIAA Aerospace Sciences Meeting; Reno, Nevada, 2007.
58. Hill GA, Thomas RH. Challenges and opportunities for noise reduction through advanced aircraft propulsion airframe integration and configurations. 8th CEAS Workshop: Aeroacoustics of New Aircraft and Engine Configurations; Budapest, Hungary, 2004.
59. Hill GA, Brown SA, Geiselhart KA, Burg CM. Integration of propulsion-airframe-Aeroacoustic technologies and design concepts for a quiet blended-wing-body transport, AIAA-2004-6403. 4th Aviation Technology, Integration and Operations (ATIO) Forum; Chicago, IL, 2004.
60. Nickol CL, Haller WJ. Assessment of the performance potential of advanced subsonic transport concepts for NASA's Environmentally Responsible Aviation Project, AIAA 2016-1030. 54th AIAA Aerospace Sciences Meeting; January 4-8; San Diego, CA, 2016.
61. Thomas RH, Burley CL, Guo Y. Progress of aircraft system noise assessment with uncertainty quantification for the Environmentally Responsible Aviation Project, AIAA-2016-3040. 22nd AIAA/CEAS Aeroacoustics Conference; Lyon, France, 2016.
62. Thomas RH, Burley CL, Olson ED. Hybrid wing body aircraft system noise assessment with propulsion airframe aeroacoustic experiments. International Journal of Aeroacoustics. 2012;11(3+4):369-410.
63. Nickol CL, McCullers LA. Hybrid wing body configuration system studies, AIAA-2009-931. 47th AIAA Aerospace Sciences Meeting; Orlando, FL, 2009.
64. Czech MJ, Thomas RH, Elkoby R. Propulsion airframe aeroacoustic integration effects for a hybrid wing body aircraft configuration. International Journal of Aeroacoustics. 2012;11(3+4):335-68.
65. Thomas RH, Burley CL, Nickol CL. Assessment of the noise reduction potential of advanced subsonic transport concepts for NASA's Environmentally Responsible Aviation Project, AIAA 2016-0863. 54th AIAA Aerospace Sciences Meeting; San Diego, CA, 2016.
66. Bonet JT, Schellenger HG, Rawdon BK, Elmer KR, Wakayama SR, Brown D, et al. Environmentally Responsible Aviation (ERA) Project - N+2 advanced vehicle concepts study and conceptual design of subscale test vehicle (STV). NASA, 2013 CR 2013-216519.
67. Guo Y, Burley CL, Thomas RH. Landing gear noise prediction and analysis for tube-and-wing and hybrid wing body aircraft, AIAA-2016-1273. 54th AIAA Aerospace Sciences Meeting; San Diego, CA, 2016.
68. Guo Y, Burley CL, Thomas RH. Modeling and prediction of Krueger device noise, AIAA-2016-2957. 22nd AIAA/CEAS Aeroacoustics Conference; Lyon, France, 2016.
69. Thomas RH, Czech MJ, Doty MJ. High bypass ratio jet noise reduction and installation effects including shielding effectiveness. 51st AIAA Aerospace Sciences Meeting; Grapevine, TX, 2013.
70. Doty MJ, Brooks TF, Burley CL, Bahr CJ, Pope DS. Jet noise shielding provided by a hybrid wing body aircraft, AIAA-2014-2625. 20th AIAA/CEAS Aeroacoustics Conference; Atlanta, GA, 2014.
71. Hutcheson FV, Brooks TF, Burley CL, Bahr CJ, Stead DJ, Pope DS. Shielding of turbomachinery broadband noise from a hybrid wing body aircraft configuration, AIAA-2014-2624. 20th AIAA/CEAS Aeroacoustics Conference; Atlanta, GA, 2014.
72. McCullers LA. Aircraft configuration optimization including optimized flight profiles. Proceedings of the Symposium of Recent Experiences in Multidisciplinary Analysis and Optimization, NASA CP 2327 (Part I). Hampton, VA, : NASA; 1984. p. 395-412.
73. Ozoroski TA. Description, usage, and validation of the MVL-15 modified vortex lattice analysis capability. Hampton, VA, : NASA, 2015 CR-2015-218969.
74. Lytle JK. The Numerical Propulsion System Simulation: An overview. Cleveland, OH, : NASA, 2000 TM-2000-209915,.
75. Tong MT, Naylor BA. An object-oriented computer code for aircraft engine weight estimation, GT2008-50062. ASME Turbo-Expo; Berlin, Germany, 2008.
76. Rizzi SA, Christian A. A psychoacoustic evaluation of noise signatures from advanced civil transport aircraft, AIAA-2016-2907. 22nd AIAA/CEAS Aeroacoustics Conference; May 30 - June 1; Lyon, France, 2016.
77. Maglieri DJ, Bobbitt PJ, Plotkin KJ, Shepherd KP, Coen PG, Richwine DM. Sonic boom, Six decades of research (SP-2014-622). Hampton, VA, : NASA; 2014.
78. McLean FE. Some non-asymptotic effects on the sonic boom of large airplanes. NASA, 1965 TND-2877.
79. Whitham GB. The behavior of supersonic flow past a body of revolution far from the axis. Proceedings of the Royal Society A. 1950 March;201(1064):89-109.
80. Whitham GB. The flow pattern of a supersonic projectile. Communications on Pure and Applied Math. 1952 August;V(3):301-48.
81. Walkden F. The shock pattern of a wing-body combination, far from the flight path. The Aeronautical

Quarterly. 1958;IX:164-94.
82. Seebass R, George AR. Sonic-boom minimization. Journal of the Acoustical Society of America. 1972;51(2):686-94.
83. George AR, Seebass R. Sonic boom minimization including both front and rear shocks. AIAA Journal. 1971;9(10):2091-3.
84. Park MA, Morgenstern JM. Summary and statistical analysis of the First AIAA Sonic Boom Prediction Workshop, AIAA-2014-2006. 32nd AIAA Applied Aerodynamics Conference; Atlanta, GA, 2014.
85. Page J, Plotkin KJ. An efficient method for incorporating computational fluid dynamics into sonic boom prediction, AIAA-91-3275. 9th Applied Aerodynamics Conference; Baltimore, MD, 1991.
86. George AR. Reduction of sonic boom by azimuthal redistribution of overpressure, AIAA-68-159. 6th Aerospace Sciences Meeting; New York, NY, 1968.
87. Page J, Plotkin KJ, Wilmer C. PCBoom version 6.6: Technical reference and user manual, Wyle Report WR 10-10. Arlington, VA, : Wyle Laboratories, 2010.
88. Rallabhandi SK. Advanced sonic boom prediction using the augmented Burgers equation. Journal of Aircraft. 2011;48(4):1245-53.
89. Plotkin KJ. State of the art of sonic boom modeling. Journal of the Acoustical Society of America. 2002;111(1):530-6.
90. Haering Jr. EA, Murray JE, Purifoy DD, Graham DH, Meredith KB, Ashburn CE, et al. Airborne Shaped Sonic Boom Demonstration pressure measurements with computational fluid dynamics comparisons, AIAA-2009-9. 43 AIAA Aerospace Sciences Meeting; Reno, NV, 2005.
91. Thomas C. Northrop-Grumman Corporation's modified U.S. Navy F-5E Shaped Sonic Boom Demonstration (SSBD) aircraft, Photo No. EC03-0210-1: NASA; 2003. Available from: www.drfc.nasa.gov/Gallery/Photo/index.html.
92. Leatherwood JD, Shepherd KP, Sullivan BM. A new simulator for assessing subjective effects of sonic booms. Hampton, VA, : NASA, 1991 TM 104150.
93. Leatherwood JD, Sullivan BM, Shepherd KP, McCurdy DA, Brown SA. Summary of recent NASA studies of human response to sonic booms. Journal of the Acoustical Society of America. 2002;111(1).
94. Leatherwood JD, Sullivan BM. Laboratory study of effects of sonic boom shaping on subjective loudness and acceptability. Hampton, VA, : NASA, 1992 TP-3269.
95. Klos J. Overview of an indoor sonic boom simulator at NASA Langley Research Center. InterNoise 2012 New York, NY, 2012. p. 8973–83.
96. Naka Y. Subjective evaluation of loudness of sonic booms indoors and outdoors. Acoustical Science and Technology. 2013;34(3):225-8.
97. Loubeau A, Naka Y, Cook BG, Sparrow VW, Morgenstern JM. A new evaluation of noise metrics for sonic booms using existing data. 20th International Symposium on Nonlinear Acoustics including the 2nd International Sonic Boom Forum; Lyon, France, 2015.
98. Rathsam J, Loubeau A, Klos J. A study in a new test facility on indoor annoyance caused by sonic booms. Hampton, VA,: NASA, 2012 TM–2012-217332.
99. Loubeau A, Sullivan BM, Klos J, Rathsam J, Gavin JR. Laboratory headphone studies of human response to low-amplitude sonic booms and rattle heard indoors. Hampton, VA, : NASA, 2013 TM-2013-217975.
100. Rathsam J, Loubeau A, Klos J. Simulator study of indoor annoyance caused by shaped sonic boom stimuli with and without rattle augmentation. Noise-Con 2013; Denver, CO, 2013.
101. Rathsam J, Loubeau A, Klos J. Effects of indoor rattle sounds on annoyance caused by sonic booms. Journal of the Acoustical Society of America. 2015;138(1):EL 43-8.
102. Geiselhart KA, Ozoroski LP, Fenbert JW, Shields EW, Li W. Integration of multifidelity multidisciplinary computer codes for design and analysis of supersonic aircraft, AIAA-2011-465. 49th AIAA Aerospace Sciences Meeting; Orlando, FL, 2011.
103. Rallabhandi SK, Nielson EJ, Diskin B. Sonic-boom mitigation through aircraft design and adjoint methodology. Journal of Aircraft. 2014;51(3):502-10.